Journal of
Composites Science

MDPI

Article

Mechanical Properties of Natural Jute Fiber-Reinforced Geopolymer Concrete: Effects of Various Lengths and Volume Fractions

Abdulrhman Dhaif Allah Abdo Mohammed [1,*], Wang Ronghui [1] and Ghasan Fahim Huseien [2,3,*]

[1] Department of Civil Engineering, School of Civil Engineering and Transportation, South China University of Technology, Guangzhou 510640, China; rhwang2002@163.com
[2] Guangzhou Institute of Energy Conversion, Chinese Academy of Sciences, Guangzhou 510640, China
[3] Department of the Built Environment, School of Design and Environment, National University of Singapore, Singapore 117566, Singapore
* Correspondence: 567dhaif@gmail.com (A.D.A.A.M.); eng.gassan@yahoo.com (G.F.H.); Tel.: +65-83057143 (G.F.H.)

Abstract: Enhancing the fracture strength and ductility of concrete through the incorporation of various types of synthetic and natural fibers with varying textures and contents remains challenging. Natural fibers, being versatile and eco-friendly construction materials, can be an excellent alternative to synthetic fibers. However, studies on natural fiber-reinforced (especially through the incorporation of jute fibers) novel composites like geopolymer binders remain deficient. Thus, the effects of various lengths (15, 25 and 35 mm) and volume contents (0.10, 0.20, 0.30, 0.40, 0.50, 0.60, and 0.70%) of natural jute fibers on the mechanical performance of fiber-reinforced geopolymer concrete were studied. The results revealed that jute fiber reinforcement remarkably affected the workability, compressive strength, fracture strengths, water absorption and microstructure properties of the proposed geopolymer concretes. Increasing the fiber length and volume fractions in the geopolymer matrix lowered the slump values and workability and increased the compressive strength. The specimen prepared with a fiber length of 35 mm and volume fractions of 0.70% displayed the lowest slump value (28 mm) and highest compressive strength (31.5 MPa) at 28 days. In addition, the specimens made with fiber volume fractions of 0.10, 0.20, 0.30, and 0.40% showed a significant improvement in the splitting tensile and flexural strengths. However, increasing the volume of the jute fibers up to 0.50% led to a slight drop in the fracture strength of the geopolymers. The specimens prepared with a length of 25 mm and a volume of 0.40% achieved the highest enhancement of splitting tensile strength (18.7%) and flexural strength (29.1%) at 28 days. In short, sustainable geopolymer concrete with high fracture performance can be obtained by incorporating natural jute fibers, leading to practical applications in the construction sector. The proposed green concrete may enable a reduction in solid waste, thus promoting a more sustainable concrete industry.

Keywords: reinforced geopolymer concretes; natural jute fibers; fracture strength; high-volume fly ash

Citation: Mohammed, A.D.A.A.; Ronghui, W.; Huseien, G.F. Mechanical Properties of Natural Jute Fiber-Reinforced Geopolymer Concrete: Effects of Various Lengths and Volume Fractions. *J. Compos. Sci.* **2024**, *8*, 450. https://doi.org/10.3390/jcs8110450

Academic Editors: Xiangfa Wu and Oksana Zholobko

Received: 8 October 2024
Revised: 21 October 2024
Accepted: 25 October 2024
Published: 1 November 2024

1. Introduction

The use of concrete with little or no cement has emerged as a popular approach in mitigating the effects of environmental pollution and climate change. Concrete free of cement, commonly known as geopolymer concrete, is produced by blending materials based on aluminosilicates [1,2]. Various wastes such as fly ash (FA) [3], ground-blast furnace slag (GBFS) [4], and palm oil fuel ash (POFA) [5], activated with alkaline solutions, are frequently utilized in the production of geopolymers [6–8]. Various binders composed of low amounts of calcium, like metakaolin (MK) [9] and class F FA [10], are mainly preferred for producing geopolymer composites. However, the application of MK has been limited in

recent years due to the high temperature requirement for manufacturing and great demand for hydration liquids [11]. FA, being a by-product, is regarded as a good aluminosilicate source and does not require energy-intensive production processes [12,13]. Nevertheless, the extended setting time and the requirement for high-temperature curing are significant drawbacks of FA-based geopolymers. Typically, FA is activated in the temperature range of 60–100 °C for about 24 to 28 h [14], as FA particles have low reactivity at ambient temperatures, limiting their use primarily to the precast system. Earlier investigations have demonstrated that partial replacement of FA with 10 to 50% of GBFS can be effective to surmount these challenges, resulting in elevated strength compared to geopolymers made from FA only [15–17].

In recent years, geopolymer composites have gained increasing attention as environmentally friendly alternatives to traditional cement. These materials possess desirable characteristics such as lower greenhouse gas emissions and energy usage, high resistance to fire and flame, as well as superior compressive strength and durability [18,19]. However, one of the key limitations of geopolymer composites is their relatively low flexural and tensile strength [20,21]. Additionally, their resistance to cracking is lower compared to conventional concrete [21]. In concrete structures, cracks facilitate the penetration of water and corrosive materials such as sulfate and chloride, which can degrade the material's durability over time [22,23]. To address this, fiber reinforcement has been widely employed to improve the mechanical properties of geopolymer concrete [24]. Various natural and synthetic fibers and steel were employed in reinforcing GPC and mitigating the propagation of cracks in the material [25–28]. Yan et al. [29] acknowledged that the cracks in fiber-reinforced geopolymers are deflected and arrested by the fibers when subjected to load, effectively preventing the cracks from propagating. The stress within the geopolymer matrix is partially absorbed by the fibers, and residual stress is transferred to the unfractured location, allowing the formation of multiple micro-cracks. Geopolymers reinforced with fibers demonstrate notable strength and stability in relation to water permeability [30], drying shrinkage [31], and resistance to abrasion [32,33]. The strength and longevity of fiber-reinforced geopolymers are influenced by factors such as the types of fiber and their properties, aspect ratios (length to diameter), contents, the nature of the matrix, the curing age and the condition of the composite [26]. Nonetheless, the adhesion of fibers in the geopolymer matrix is critical in determining their durability and strength performance [20]. Robust interfaces can facilitate effective load transfer from the composite matrix to fiber networks with high load-bearing capacity, while fibers having inert surfaces result in weak coupling at the matrix–fiber interface, leading to de-bonding failures in the composite [34,35].

Over the past few decades, various fibers, including steel and fibers (natural and synthetic), were examined for their use in a brittle geopolymer matrix [36,37]. However, these materials present challenges, such as high costs and considerable environmental impacts [38]. Data indicate that the construction sector accounts for 36% of global CO_2 emissions and approximately 40% of the European Union's total energy consumption. Consequently, the industry, along with material manufacturers, must make concerted efforts to apply the "3Rs" principles—reduce, reuse, and recycle. By incorporating more environmentally friendly materials from supportable raw substances into fiber production, the emission of CO_2 and energy usage can be lowered [39–41]. In short, as a sustainable substitute to synthetic fibers, natural fibers have become interesting due to their cost-effectiveness and ease of handling. Furthermore, natural fibers, sourced from renewable materials, pose minimal environmental risks [42,43].

Jute is a natural fiber derived from the Corchorus plant. This vegetable fiber is long, soft, and shiny, and it can be spun into coarse, strong threads. After cotton, jute is the most commonly used natural fiber [44,45]. Jute fiber is extracted from the stem and outer skin (ribbon) of the plant using retting and stripping techniques. It is commonly used in the production of items such as rope, twine, and rush matting, which is also used to control flood erosion. By contrast, cement concrete is brittle, has low tensile strength, limited resistance

to crack initiation and propagation, and only moderate elongation at break [46–48]. In recent years, there has been a continuous effort to incorporate jute fibers into conventional vibrated concrete as part of the global movement toward sustainability [49–51]. Zakaria et al. [52] explored how different lengths (10, 15, 20, and 25 mm) and concentrations (0.1%, 0.25%, 0.50%, and 0.75% by weight) of jute fibers affect the characteristics of vibrated concretes. It was found that the addition of 0.25% jute fibers of 15 mm length can significantly enhance the strength performance of concrete, wherein there is a 35% enhancement of the tensile strength compared with the control specimen. Islam and Ahmed [49] examined the effects of varying the volume fractions (0.1%, 0.30%, and 0.50%) at a fixed length (20 mm) of jute fibers reinforcement in concrete, achieving higher resistance against crack formation compared to normal concrete. Kim et al. [53] studied the mechanical properties of jute fiber-reinforced concrete and observed significant improvements in the strength performance compared to standard specimen. However, recent studies on eco-friendly high-volume fly ash geopolymer incorporating natural fibers, particularly jute fiber, remain scarce.

The background outlined above indicates that fiber-reinforced geopolymer concrete offers several potential advantages. It suggests that the adhesion of fibers to the concrete matrix is a key factor influenced by the uniform dispersion of fibers within the composite network. Achieving uniform distribution requires accurately predicting the optimal fiber content and length to produce geopolymer composites with enhanced durability and strength performance. Despite some research efforts, the current knowledge regarding the impact of varying the fibers' length and volume fractions on the overall characteristics of fiber-reinforced geopolymer composites remains limited. In this perception, we explored the possibility of developing a new type of geopolymers by embedding jute fibers into the concrete matrix, aiming to improve the fracture performance and ductility, particularly the splitting tensile and flexural strength of the modified concrete. The effects of different volume fractions (0.10%, 0.20%, 0.30%, 0.40%, 0.50%, 0.60%, and 0.70%) and lengths (15 mm, 25 mm, and 35 mm) of natural jute fibers on the workability and mechanical properties were evaluated. Tests conducted include slump, compressive strength, splitting tensile strength, flexural strength, modulus of elasticity, and water absorption. Additionally, the microstructural properties of the composites were analyzed using microscopic and spectroscopic techniques.

2. Materials and Methods

2.1. Materials Characterization

The geopolymer concrete specimens were made using a high volume of (75%) low-calcium FA (Class F) and GBFS (25%). Figure 1 displays the XRF results for the elemental compositions of GBFS and FA, meeting ASTM C618 standard. The primary compounds in FA were silica oxide (SiO_2), aluminum oxide (Al_2O_3), and iron oxide (Fe_2O_3) at 56.82, 25.11, and 8.82%, respectively. These oxides of SiO_2, Al_2O_3, and Fe_2O_3 contributed more than 90.75% of the FA chemical composition, while for GBFS, the primary compounds are calcium oxide (CaO), SiO_2, and Al_2O_3 at 49.63, 31.17, and 12.87%, respectively. Compared to GBFS (49.63%), the content of CaO in the FA sample was very low (5.14%). However, the content of magnesium oxide (MgO) and sodium oxide (Na_2O) were higher (4.38 and 0.39%) compared to the FA (1.36 and 0.04%). Both FA and GBFS display very low percentage (0.12 and 0.18%) of loss on ignition (LOI) and in the range of limitation. The physical properties of FA and GBFS were also evaluated. The medium particles size was found to be 10 µm for FA and 12.4 µm for GBFS. FA presented a light gray color, which was in contrast to the off-white color of GBFS. Additionally, FA demonstrated a higher specific surface area (18.2 m^2/g) compared to GBFS (13.6 m^2/g).

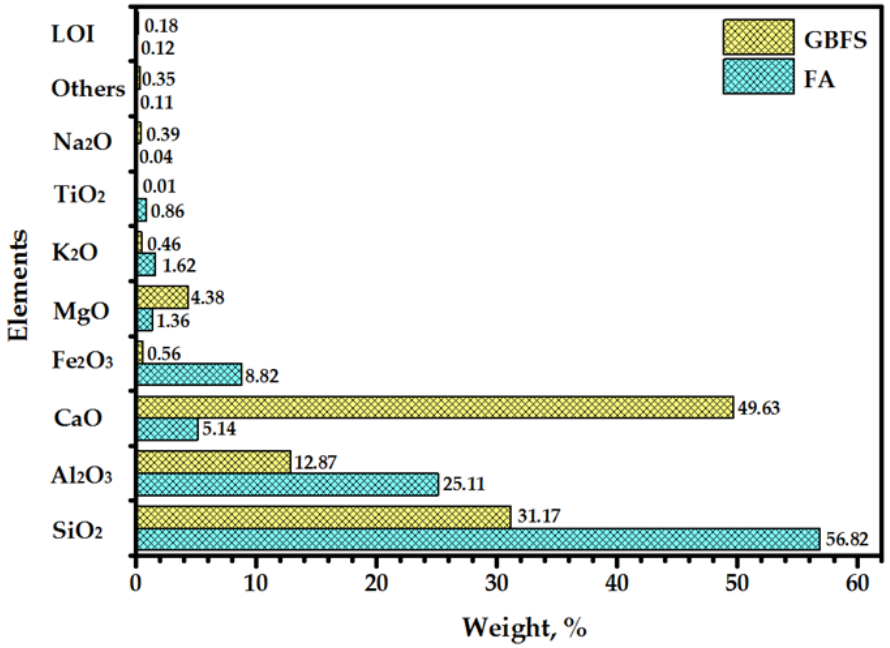

Figure 1. Compositions of FA and GBFS.

The alkaline activator solution (AAS) was composed of NaOH (NH) and sodium silicate (NS). This solution was made for activating the geopolymers. Pure NaOH (98% purity) in pellet form supplied by a local company (China) was used to make the alkali solutions (6M) by dissolving these pellets in water at a 1:4.15 ratio. Then, the produced NH solution was allowed to cool for 24 h and mixed with the NS mixture to obtain the final alkali solution for the activation of geopolymers [54]. The alkali solution was used in two parts with an NH to NS ratio of 1:2.5. Figure 2 illustrates the procedures for making the alkali activator solution in two parts.

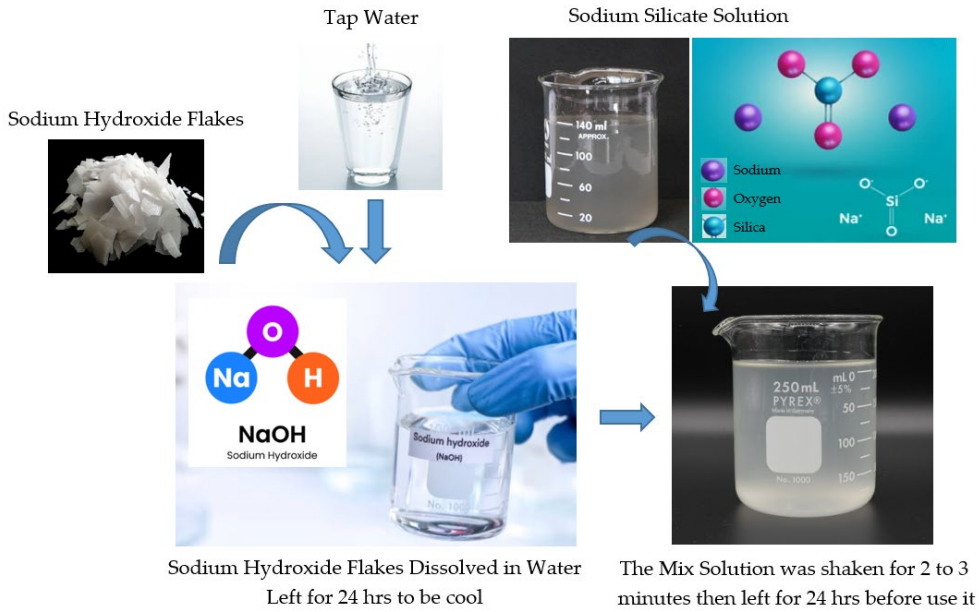

Figure 2. Protocols of alkali activator solutions preparation (two parts).

Natural jute fibers were obtained from the local supplier in China as raw natural fibers for preparing the reinforced geopolymer concrete' specimens. The fibers were extracted from the plant using water retting and were supplied in lengths ranging from 50 to 120 mm. Natural fiber-based composites have a high amount of moisture absorption and weak

adhesion amid fibers and the binder matrix, leading to the formation of voids around the fibers and thus a weaker composite structure. To improve the properties and performance of the received jute fibers, they were chemically treated in alkaline mixture prior to use. Following the previous research [55,56], a 4% NH solution was utilized in treating these jute fibers (Figure 3). Prior to the alkali treatment of these natural fibers, they were rinsed and combed to remove the contaminants followed by cutting into small segments 30 to 75 mm long, facilitating the entire treatment. The cleaned and segmented fibers were immersed in alkaline mixture for an optimal duration of approximately 3 h, ensuring the prevention of fiber degradation. After treatment, the fibers were washed and soaked with water for a day before being oven-dried at 80 °C for 6 h [57]. Once dried, the fibers were subjected to various tests to evaluate their strengths, density and diameters, as the quantity of fibers embedded in the geopolymer binders depends on their volumetric ratio and density. After conducting the necessary tests, the jute fibers were cut to lengths of 15 mm, 25 mm, and 35 mm for use in the geopolymer mixtures (Figure 4).

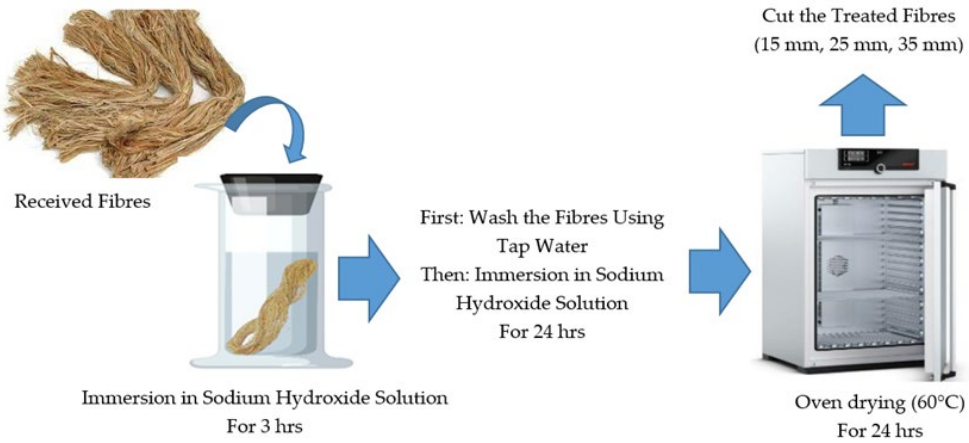

Figure 3. Lab treatment for the received jute fibers before use in geopolymer concrete preparation.

Figure 4. Used lengths of fibers in preparation of geopolymer concrete specimens.

Figure 5 shows the sieving analysis results of river sand and crushed stone. River sand with a nominal maximum size of 4.75 mm was used as the fine aggregate. The sand, which was well graded, had a specific gravity of 2.6. The proper grading of these aggregates was essential to minimize the demand of water in the geopolymer matrix, preventing their segregations in the mixing process. In addition, these aggregates were cleaned to eliminate any organic matters and impurities. In all mixes, crushed granites (coarse aggregates) of particle sizes below 10 mm with 2.7 of specific gravity were employed. The sieve size of most of the coarse aggregates ranged from 4.75 to 10 mm. The grading of coarse aggregate was vital due to their strong influence on the segregations and balling performance together

with the surface areas alteration of fiber-reinforced binders. Researchers revealed that coarse aggregates with poor grading can negatively impact various salient characteristics of the resultant concrete.

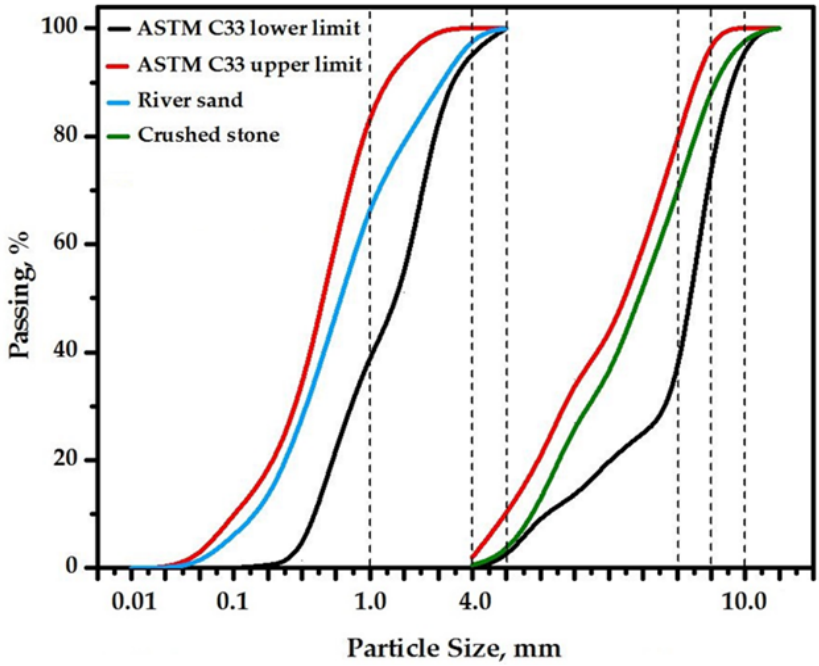

Figure 5. Outcomes of river sand and crushed stones' sieving analysis.

2.2. Mix Design and Preparation of Composites

The proposed jute fiber-reinforced geopolymer concrete mixes and their proportions are presented in Table 1. In preparing the proposed jute fiber-reinforced geopolymer concrete, FA and GBFS were blended for two minutes for achieving a homogeneous binary binder. The capacity of the mixer drum was 0.18 m^3, which ensured a uniformity in the concrete mix. Initially, 50% of the coarse and fine aggregates were mixed for two minutes, followed by the addition of the remaining 50%, which was mixed for an additional three minutes while the materials remained dry. Subsequently, the binary blended binder composed of FA and GBFS was incorporated. All materials, including the dry binder, coarse and fine aggregate were combined for three minutes followed by alkali solution activation (75% of two-part of alkaline activated solution) and mixing for another 2 min. Upon the wet mixing, the natural jute fibers were spread into the mixture while the mixing process continued. The activated mixtures were then mixed for an additional three minutes prior to the measurement of slump values. Later, the obtained mix was poured into pre-prepared steel molds in accordance with ASTM C579-18 [58]. In accordance with ASTM C143 [59], the workability values of the fresh fiber-reinforced specimens were assessed by slump testing. Cubical molds measuring 70 mm × 70 mm × 70 mm, cylinders 100 mm × 200 mm, and beams 100 mm × 100 mm × 500 mm were used to prepare the concrete specimens. All molds were washed thoroughly to remove any impurities and residues. The fiber-reinforced geopolymer concrete mixture was dispensed into the cleaned mold layer by layer, wherein every layer was subjected to a vibration table for the compaction, ensuring minimum air pockets. Next, each mold surface was flattened with the floating of plasterers. The obtained concrete mixes were kept under laboratory conditions at 30 ± 1.5 °C and over 80% of relative humidity for 24 h before being demolded and kept in the lab condition until the test time after 7 and 28 days of aging. The procedure of preparing the proposed geopolymer concrete specimens is illustrated in Figure 6.

Table 1. Mix of natural jute fiber-reinforced geopolymer concretes.

Concrete Codes	Jute Fibers			Binder (B), kg/m^3		Aggregates, kg/m^3		Alkaline Solution, kg/m^3		
	L, mm	Vol., %	Weight, kg/m^3	FA	GBFS	Fine	Coarse	AAS:B	NH	NS
J0-0	0	0	0	464	176	684	910	0.50	91.4	228.6
J15-0.1	15	0.10	0.43	464	176	684	910	0.50	91.4	228.6
J15-0.2		0.20	0.86							
J15-0.3		0.30	1.30							
J15-0.4		0.40	1.73							
J15-0.5		0.50	2.16							
J15-0.6		0.60	2.59							
J15-0.7		0.70	3.02							
J25-0.1	25	0.10	0.43	464	176	684	910	0.50	91.4	228.6
J25-0.2		0.20	0.86							
J25-0.3		0.30	1.30							
J25-0.4		0.40	1.73							
J25-0.5		0.50	2.16							
J25-0.6		0.60	2.59							
J25-0.7		0.70	3.02							
J35-0.1	35	0.10	0.43	464	176	684	910	0.50	91.4	228.6
J35-0.2		0.20	0.86							
J35-0.3		0.30	1.30							
J35-0.4		0.40	1.73							
J35-0.5		0.50	2.16							
J35-0.6		0.60	2.59							
J35-0.7		0.70	3.02							

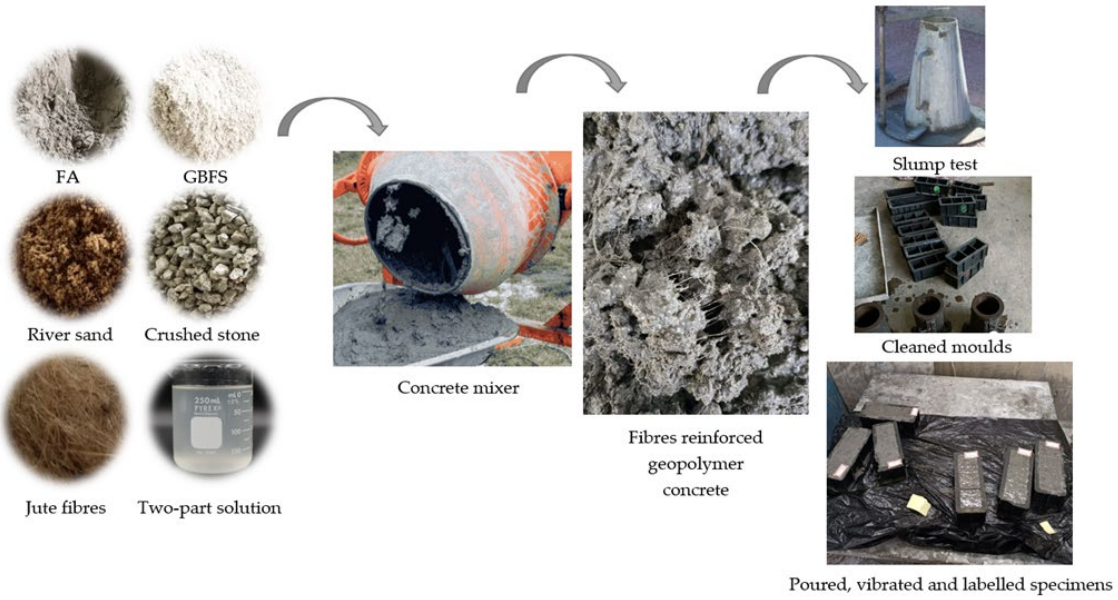

Figure 6. Jute fiber-reinforced geopolymer concrete specimens' preparation.

2.3. Procedures of Tests

Slump tests (following BS EN 12350–2 standards [60]) were performed to determine the workability of geopolymer concrete. Fresh control and reinforced specimens were placed in the slump cone, which was followed by three stages of compaction using a rod. The slump was measured as the vertical distance between the top of the rod and the midpoint of the concrete's surface. Geopolymer concrete specimens prepared without jute fibers served as control samples to assess the impact of the jute fiber length and volume fractions on the strength properties of the proposed geopolymer concrete. Three kinds of specimens for each mixture were made into cubes, cylinders, and beams measuring (70 mm × 70 mm × 70 mm), (100 mm × 200 mm), and (100 mm × 100 mm × 500 mm), respectively. Following the casting process, the specimens were kept at an ambient temperature of 26. The average values from three specimens at curing ages of 7 and 28 days were used to evaluate the strength performance, including compressive strength (CS), splitting tensile strength (STS), flexural strength (FS), and modulus of elasticity (MOE), and an automatic machine with a maximum load of 3000 kN was used. A constant rate of loading (5 kN/s) applied to the failure of the tested specimens. The flexural strength test was carried out using the universal testing machine that is used for the determination of the concrete compressive and splitting tensile strength with a rate 0.2 kN/s rate of loading. The CS of concrete was measured following BS EN 12390–3 [61] on 70 mm cubes with CS tests conducted on specimens cured for 7 and 28 days. The STS tests adhered to the BS EN 12390–6 standards [62]. The FS tests followed the standard of BS EN 12390-5 [63]. The specimens' MOE tests were performed in accordance with the standard of ASTM-C469 [64]. Water absorption tests were carried out according to ASTM C642 [65]. At every curing age, the measurement was performed on 3 samples to obtain the mean value. The microstructures of specimens were analyzed by crushing them, wherein the central part of every specimen was tested using Field Emission Scanning Electron Microscopy (FESEM). In addition, several tests such as X-ray diffraction (XRD), differential thermogravimetry, Fourier-transform infrared spectroscopy (FTIR) and FESEM were conducted on the binary blends of FA-GBFS after activation by 6 M of the two-part alkali solution to measure the change in chemical composition and surface morphology compared to the raw materials (FA and GBFS).

3. Results and Discussion

3.1. Fibers' Salient Characteristics

The physical and engineering attributes of treated natural jute fibers were evaluated in terms of diameter, density, elongation break percentage, ultimate tensile strength, stiffness and water absorption. From the conducted tests, the obtained results are illustrated in Table 2. The diameter, density, elongation, ultimate tensile strength, stiffness, and water absorption were 0.018 mm, 1.438 g/cm^3, 1.64%, 374 MPa, 13.6 kN/mm, and 3.96%, respectively. Furthermore, the cellulose, hemicelluloses, lignin, water soluble, ash, pectin, and cerolipoid comprised 67.8%, 12.4%, 15.1%, 1.8%, 1.7%, 0.7% and 0.5% of the chemical composition, respectively. The FESEM results presented in Figure 7 show that the fiber diameter and porosity (Figure 7b) were significantly influenced by sodium hydroxide treatment, and the diameter of the fibers decreased by 18 to 24% compared to untreated jute fibers (Figure 7a). The observed decrease in the jute fibers' diameter agreed with the report of Ibrahim et al. [57]. This reduction was attributed to the elimination of hemicellulose, lignin and pectin. Similar trends in the fiber diameter reduction following alkaline treatment have been observed by others. It was acknowledged [66] that the reduction in the fibers' diameter can be due to morphological changes in the fibers after alkaline treatment. Their SEM analysis showed that the fibers were not monofilaments but rather bundles coated and bonded by lignin, wherein a substantial amount of lignin was removed during the treatment in alkali solution, leading to a reduction in fiber diameter. Saha et al. [67] also observed a 23% decrease in jute fiber diameter after treatment with NH solution (4%) for half an hour at room temperature. This decrease was mainly due to the elimination of a

part of the surface contaminants along with the extraction of lignin, hemicellulose, and pectin as confirmed by earlier studies [68–72].

Table 2. Physical properties of used natural jute fibers.

Diameter, mm	Density, g/cm^3	Elongation Break, %	Ultimate Tensile Strength, MPa	Stiffness, kN/mm	Water Absorption, %
0.018	1.438	1.64	374	13.6	3.96
Color: Dark-gold		Chemical processing: NaOH (concentration of 4 M)			Source: Local

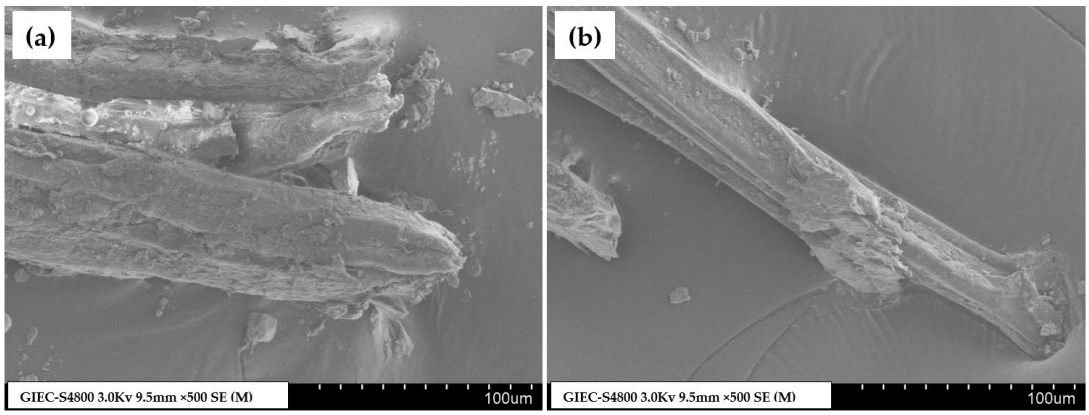

Figure 7. SEM images for longitudinal and cross-section of used fibers (**a**) before and (**b**) after treatment.

3.2. Workability of Proposed Concrete

The influence of various lengths and volume fractions of jute fibers on fresh concrete's workability is discussed widely in this section. Figure 8 shows the impact of varied length and volume fractions of jute fibers on the workability performance of the proposed geopolymer concretes. The obtained results clearly showed that the slump values can be significantly affected by the increase in the fibers' lengths and volume fractions. In Figure 8a, the effect of a 15 mm length of fiber added with a volume of 0.10, 0.20, 0.30, 0.40, 0.50, 0.60 and 0.70% on the slump value of the prepared geopolymer concretes is illustrated. An increase in the volume fractions from 0 to 0.70% leads to a decrease in slump values from 105 to 37 mm, respectively. Similar outcomes were evidenced for the fresh concrete made from various volume fractions of 25 mm fibers wherein the slump values dropped as the fiber volume fraction increased. The slump value decreased from 105 to 95, 76, 64, 47, 41, 37, and 31 mm when raising the fiber volume from 0 to 0.10, 0.20, 0.30, 0.40, 0.50, 0.60 and 0.70%, respectively. Likewise, the slump values of geopolymer concrete prepared with 35 mm fibers dropped to 89, 66, 52, 40, 35, 32, and 28 mm when increasing the fiber volume in the matrix.

In the literature, several studies [42,73] have reported that the inclusion of fibers can significantly reduce the workability by increasing the viscosity of the geopolymer mixture. Excessive fiber addition leads to reduced workability, indicating inadequate compaction [74]. As the fiber content increases, slump values decrease significantly [74,75]. Previous research has demonstrated that the incorporation of jute fibers in geopolymer concrete can considerably affect the fresh concrete's slump values [76]. A higher jute fiber content in concrete is associated with a reduction in slump, and this effect is more pronounced when using longer jute fibers compared to shorter fibers [49]. The slump value of high-fluidity concrete reinforced with jute fibers decreases more sharply than that of normal concrete [76]. Therefore, increasing the jute fibers content and fiber length in a concrete matrix has a negative impact on the slump values of fresh concretes. The slump tests were conducted [47] to examine the fresh concrete's workability after the

inclusion of jute fibers. The ratio of water to cement (w/c) was fixed (0.70) for both the control and jute fiber-reinforced specimen. The slump value of the control specimen was measured at 44 mm, while the incorporation of a 5% fiber volume fraction and length of 50 mm into the concrete could reduce the slump value to 17 mm. This observation was attributed to the decrease in the preservation and captivity effects of the jute fibers because the jute fiber-embedded concretes tend to show lower slump values than control specimen. Additionally, the high water absorption capacity of jute fibers further contributed to the slump reduction [47]. Several studies have reported similar reductions in slump with the addition of natural fibers [77–80].

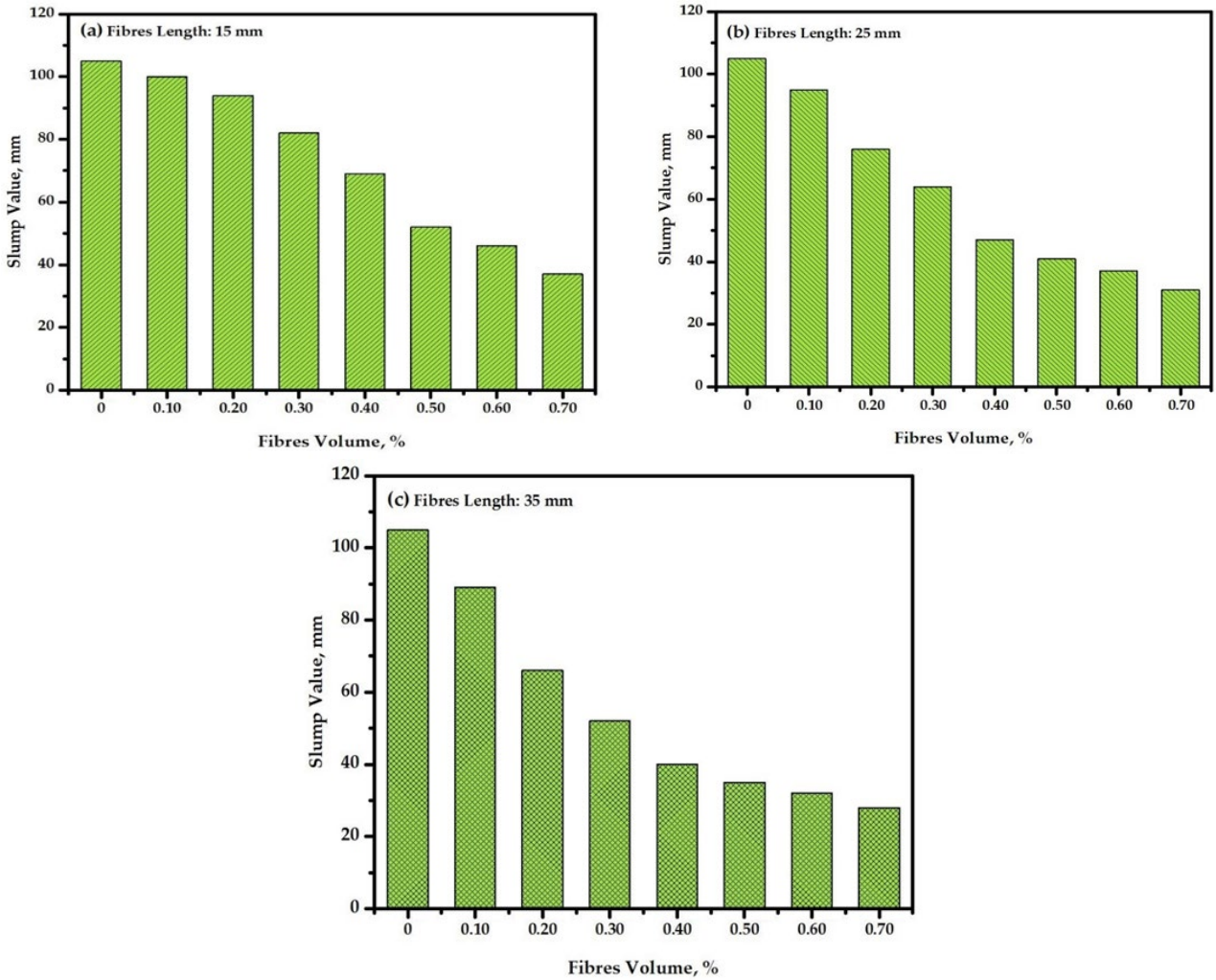

Figure 8. Effects of various volume fractions of fibers on workability performance of geopolymer concretes for (**a**) 15 mm, (**b**) 25 mm, and (**c**) 35 mm length.

Figure 9 illustrates the relationship between the proposed concrete slump readings and fiber content. It was indicated that there is an inverse relationship, and the workability of the proposed concrete tends to decrease as the fiber content in the geopolymer matrix increases. There appears to be a good correlation between the reinforced geopolymer concrete and the fiber content with a correlation coefficient of 0.84. The experimentally measured data were correlated using the linear regression technique via the following relation:

$$Concrete\ slump,\ mm = (-104.41 \times Volume\ of\ fibres) + 100.54 \quad (1)$$

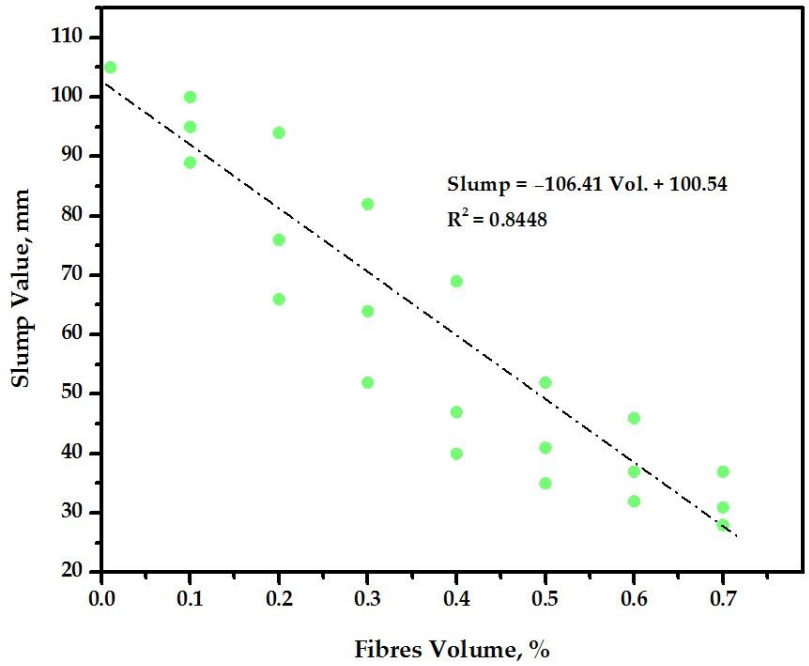

Figure 9. The relationship between the proposed concrete slump value and fiber content.

3.3. Mechanical Properties

3.3.1. Compressive Strength Development

The impact of varied lengths and volume fractions of fibers on the CS development of proposed concrete was evaluated. Figure 10 shows the obtained results of the CS of reinforced geopolymer concretes aged one and 4 weeks. The CS of the specimens increased as the curing age increased. Furthermore, the CS of the specimens was directly affected by the change in the fibers' length and volume fractions. However, the CS decreased as the fibers length and volume fractions increased in the concrete matrix. The lower strength (21.7 MPa) at early age (7 days) was found with the specimens prepared with the highest length (35 mm) and volume content (0.70%) of jute natural fibers reinforcing the geopolymers. Wongsa et al. [42] showed a decrease in the CS of geopolymer composite by 26.4 and 11.5% as the corresponding fiber volume fraction increased from 0.5 to 1.0% when coir and sisal fibers were added. For the geopolymer specimens prepared with varying volume fractions and a fixed fiber length of 15 mm (Figure 10a), the CS dropped from 37.7 to 26.1 MPa at 7 days and from 46.9 to 38.1 MPa at 28 days. Similarly, increasing the length of the fibers to 25 mm and volume fractions resulted in a significant decrease in the compressive strength values. At age of 7 days, the CS dropped from 37.7 to 24.3 MPa as the fiber volume fraction increased from 0% to 0.70%, respectively. Likewise, after 28 days, the CS dropped from 46.9 to 34.5 MPa as the fiber volume fractions increased from 0% to 0.70% (Figure 10b). Similarly, the concrete made with 35 mm fibers displayed a greater loss in compressive strength when the volume percentage of natural jute fibers included in the geopolymer matrix was higher. The results showed that increasing the volume fraction from 0.10% to 0.70% led to a drop in the compressive strength value from 34.7 to 21.7 MPa at the age of 7 days and from 44.6 to 31.5 MPa at the age of 28 days, respectively.

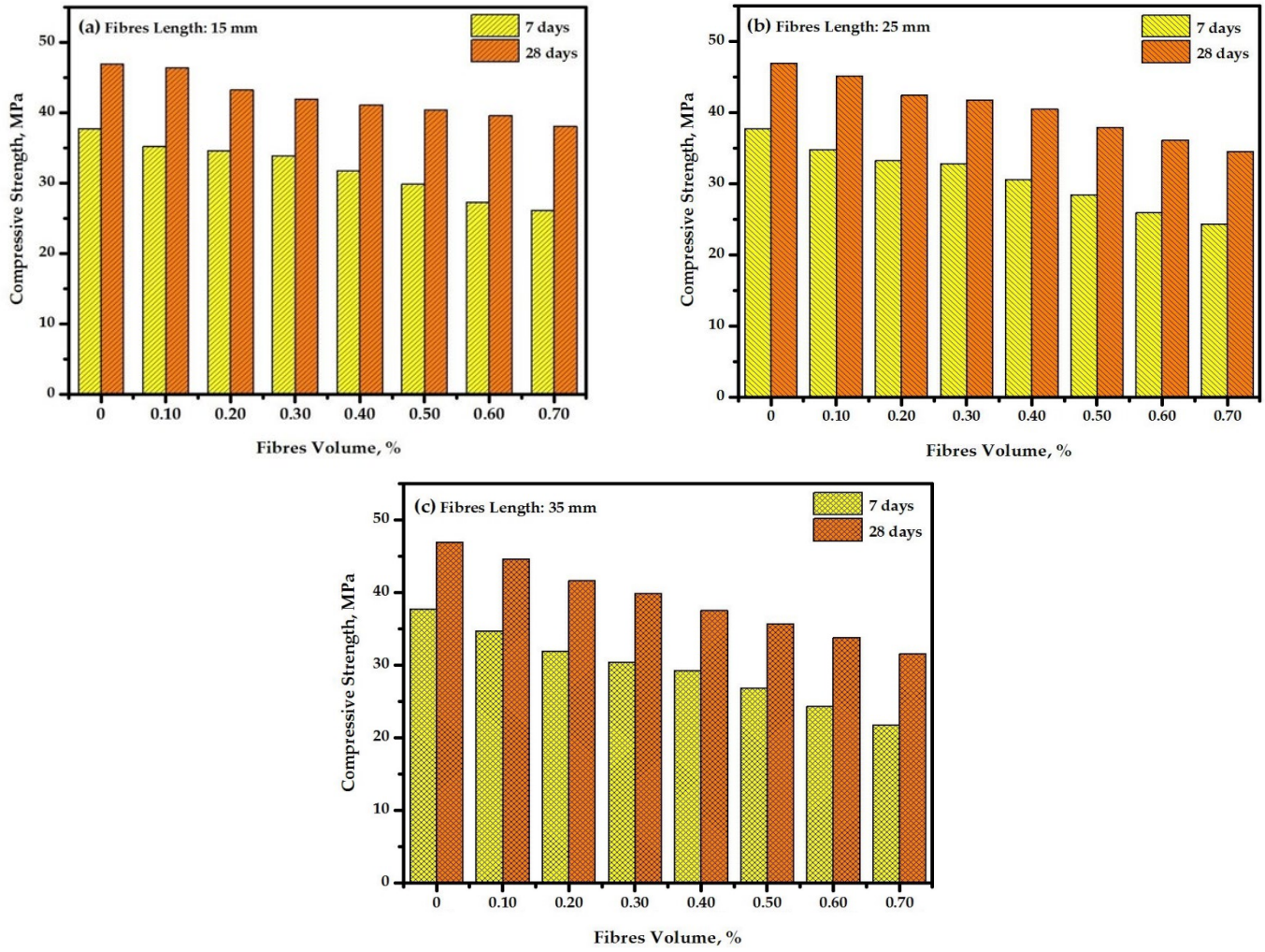

Figure 10. Impact of varying lengths and volume fractions of fibers on compressive strength development of concrete: (**a**) 15 mm (**b**) 25 mm (**c**) 35 mm.

In general, jute fiber-reinforced geopolymers with higher fiber concentrations absorb more solution, which significantly influences the geopolymerization process and leads to a reduction in compressive strength [71,81–84]. However, the optimal fiber dosage depends on various factors, including the physical properties (lengths and diameters), fiber type, mix design of concrete, and proportions of water to binder [49,50]. At lesser volume fractions of reinforced fibers, the fibers' confinement in the concrete matrix leads to a loss in compressive strength [52,84]. Conversely, at higher dosages, workability decreases, making compaction difficult and resulting in lower strength. This occurs when the addition of fibers at large volume fractions dilutes the concrete matrix, leading to a drop of CS performance [82]. The reduced compressive strength of fibrous mixtures could be explained by the presence of voids caused by the addition of jute fibers and the weak interfacial bonds between the jute fibers and FA–GBFS pastes. However, the results of this experiment indicated that the decrease in compressive strength was not substantial due to the presence of jute fibers, and the failure mode was predominantly ductile. Several types of natural fibers have been studied for the reinforcement of geopolymers, including cotton fiber [83,84], flax fiber [85], sisal fiber [42], coconut fiber [42], pine cone fiber [34], and corn fiber [86]. Most of these studies reported that the compressive strength of the designed geopolymer slightly decreased with the increase in fiber length and volume fraction.

3.3.2. Failure Modes of Proposed Concrete

Figure 11 shows how the length and volume fractions of natural jute fibers affect the failure modes of the proposed geopolymer concretes. The fibers' length (15 mm, 25 mm, and 35 mm) and volume fractions (0.10, 0.20, 0.30, 0.40, 0.50, 0.60 and 0.70%) have a significant effect on the failure modes. As known, the compressive strength for all geopolymer concrete specimens tends to decrease as the fiber volume fractions and lengths in the concrete matrix increase. Figure 11a,b show the plain and reinforced geopolymer concrete before loading, respectively. Based on the failure mode analysis, the geopolymer concrete prepared without fibers exhibits a triangular failure pattern with diagonal cracks and brittle behavior, as shown in Figure 11c. In contrast, the failure modes of natural jute fiber-reinforced geopolymer concretes, which contain varying lengths (15–35 mm) and amounts of fibers (0.10–0.70 vol.%), are generally similar, showing cracks without separation and demonstrating good ductility (Figure 11d–l). The highest ductility performance was observed with the specimens prepared with a higher volume percentage of fibers (0.70%), as shown in Figure 11f,i,l. It is important to note that despite the lower TS of the natural jute fibers compared to the synthetic ones, they are still capable of promoting fiber bridging within the geopolymer matrix and enhancing the toughness of the proposed geopolymer concrete. Visual observations further reveal that as the fiber length and content increase, the crack width decreases, evolving the crack-mediated failure of concrete from large to coarse and finally to fine with high density. The obtained findings indicated that the incorporation of jute fiber-reinforced concrete helps prevent direct vertical failure by creating fiber bridging [71]. The incorporation of fiber bridging may extend the service life of structures and provide sufficient warning before ultimate failure. The failure patterns observed in this study align with those reported in the literature [49,71,87]. Previous research shows that adding fibers to concrete limits the formation of cracks seen in concrete without any reinforcement [49]. Additionally, it was noted that cylindrical specimens without jute fiber reinforcement exhibited brittle axial fractures, while those with jute fibers developed longitudinal cracks, indicating enhanced ductility in jute fiber-reinforced concrete [49].

3.3.3. Splitting Tensile Strength

The STS analysis results of reinforced geopolymer concrete prepared with fibers with varying length and volume are illustrated in Figure 12. The STS values increased with the curing age, ranging from one to four weeks. Additionally, the inclusion of fibers in the matrix of FA-GBFS geopolymers significantly improved the tensile strength of the specimens. However, including a high volume of fibers negatively affected the performance of the tested specimens and showed lower splitting tensile strength values. As shown in Figure 12a, including 15 mm fibers with volume fractions from 0.10 to 0.70%, increasing in 0.1 increments, led to corresponding STS of 3.88, 4.08, 4.15, 4.22, 4.18, 3.98, and 3.84 MPa at 7 days of age, and 5.24, 5.37, 5.51, 5.82, 5.56, 5.47, and 5.32 MPa at 28 days of age compared to 3.74 and 5.17 MPa for the control specimens. Likewise, the specimens prepared with 25 mm fibers in a volume of 0.10, 0.20, 0.30, and 40% showed improvement in the splitting tensile strength from 3.74 to 3.96, 4.11, 4.34, and 4.58 MPa at 7 days of age and from 5.17 to 5.38, 5.63, 5.78, and 6.14 MPa at 28 days of age (Figure 12b), respectively. However, increasing the fiber volume fractions from 0.50 to 0.70% produced a drop in the corresponding STS values from 4.46 to 4.04 MPa at 7 days and from 5.86 to 5.42 MPa at 28 days. Figure 12c shows that increasing the volume fraction of 35 mm fibers from 0 to 0.10, 0.20, 0.30, and 0.40% can enhance the STS of the concrete from 3.74 to 4.06, 4.12, 4.23, and 4.27 MPa at one week of age and from 5.17 to 5.44, 5.57, 5.62, and 5.74 MPa at 4 weeks of age. However, the splitting tensile strength dropped to 4.02, 3.94, and 3.78 MPa at 7 days and to 5.59, 5.36, and 5.18 MPa at 28 days when increasing the volume percentage of fibers to 0.50, 0.60 and 0.70%, respectively. To summarize, the specimens made using 25 mm fibers at 0.40% volume fraction achieved the highest STS of 6.14 MPa compared with the control specimen (5.17 MPa), increasing by 18.7% at 28 days.

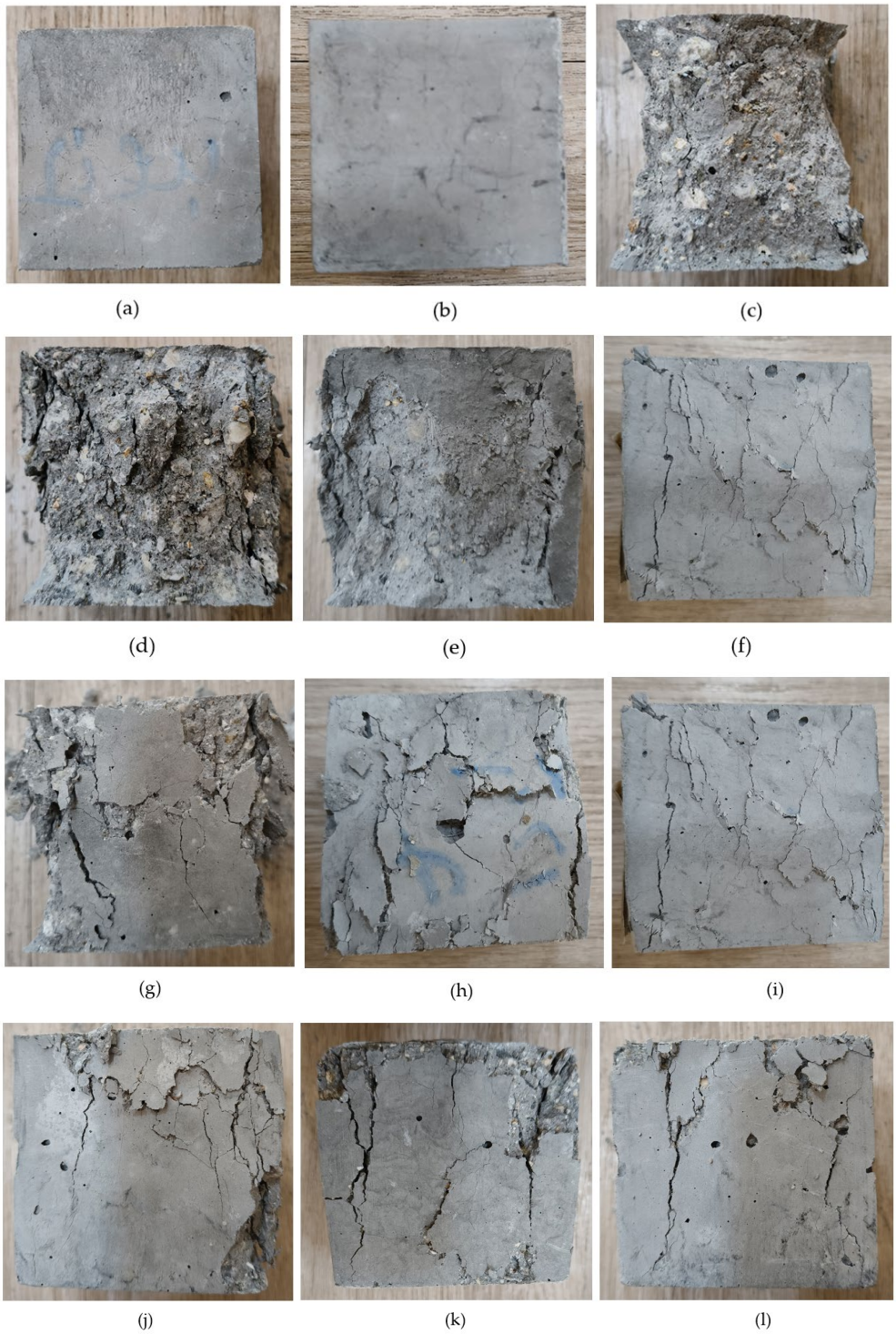

Figure 11. Effects of fiber length and volume fraction on failure mode of tested geopolymer concrete' specimens: (**a**) normal geopolymers before test, (**b**) reinforced geopolymers before test, (**c**) 0% fibers of geopolymers, (**d**) 15 mm—0.10% fibers, (**e**) 15 mm—0.40% fibers, (**f**) 15 mm—0.70% fibers, (**g**) 25 mm—0.10% fibers, (**h**) 25 mm—0.40% fibers, (**i**) 25 mm—0.70%, (**j**) 35 mm—0.10%, (**k**) 35 mm—0.40% (**l**) 35 mm—0.70%.

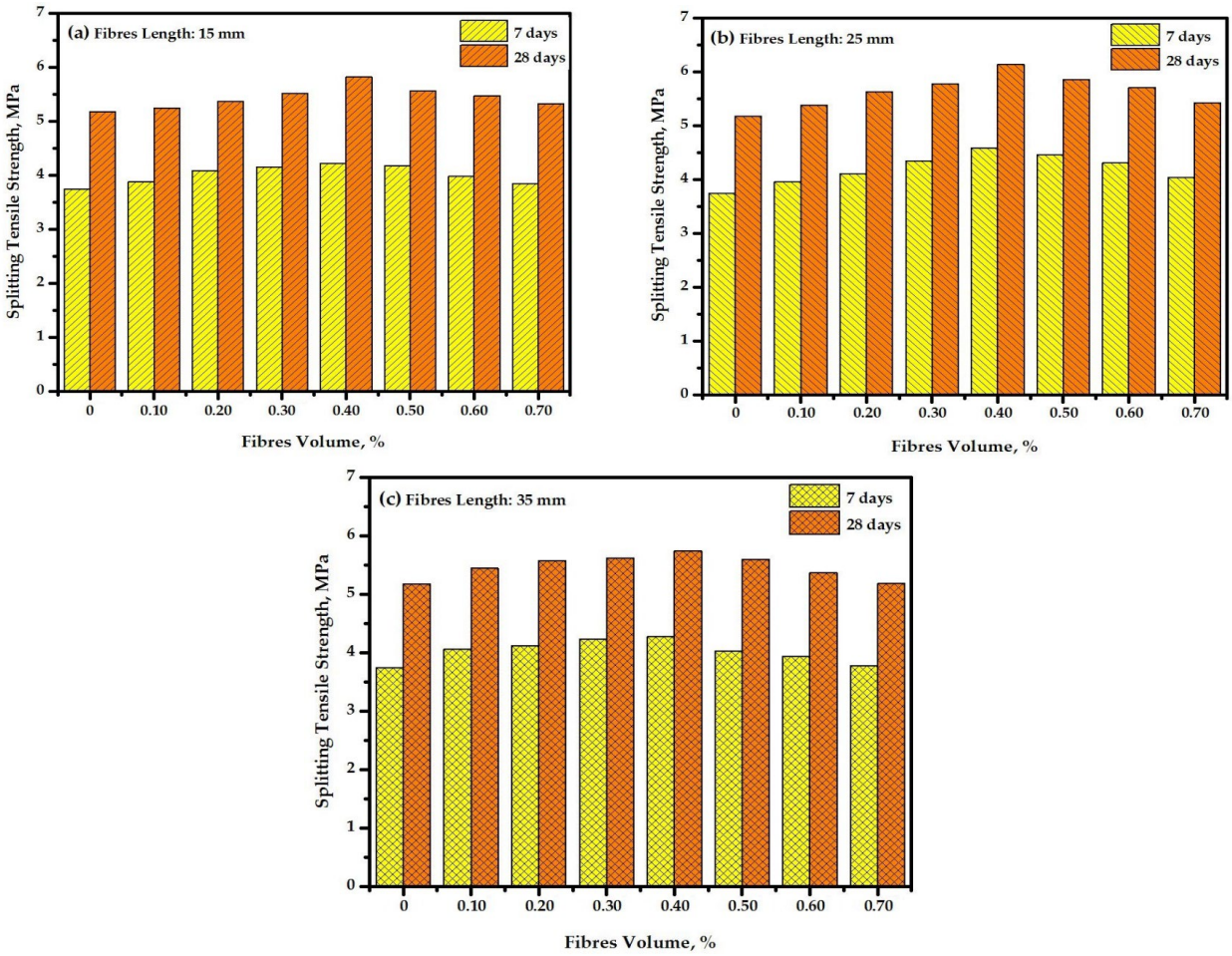

Figure 12. Fiber volume fraction-dependent STS of concretes at different lengths of (**a**) 15 mm, (**b**) 25 mm, and (**c**) 35 mm.

The improvement in the tensile strength of geopolymer specimens is largely attributed to jute fiber's ability to bond the cracks in the strain regions [38]. During splitting, the bridging of jute fibers at the crack locations allows stress transfer into the fibers from the concrete specimen, enabling the concrete to withstand the loads for a prolonged period of time. This can increase the capacity of the tensile strain of the concrete matrix, enhancing the concrete's STS [88,89]. The split tensile strength (STS) values can be influenced by variations in the fiber length and volume fraction with all mixes showing an increase in STS values at both early and later stages when fiber was incorporated into the geopolymer concrete. A similar trend was noted by Silva et al. [43], wherein the STS of geopolymer concrete made from fibers (sisal or jute) increased as the fiber volume content increased, which was followed by a drop beyond an optimal volume content of fibers. Wang et al. [90] also observed that with the increase in the basalt fibers length from 12 to 24 mm in the concrete, the STS values improved, but it was declined as the fiber length rose from 30 to 36 mm. In contrast, geopolymers incorporating longer fibers and higher volume fractions (35 mm, 0.70%) demonstrated weaker adhesion between the fibers and the composite matrix, which was characterized by larger gaps, voids, and air pockets around the fiber–matrix interface. Under load, these gaps expanded, increasing void formation, which weakened the bond and led to failure at lower fracture strength levels compared to composites containing 15 mm and 25 mm fibers or lower volume fractions. The STS of reinforced geopolymer concrete can decrease when longer fibers ($\geq$35 mm) or higher volumes (0.50–0.70%) of jute fibers are included in the mixtures due to several factors. Firstly, longer or excessive jute fibers do not distribute evenly within the geopolymer concrete matrix, leading to poor

bonding between the fibers and the matrix. This can result in gaps, voids, or weak spots around the fibers, reducing the material's overall fracture strength. Additionally, higher jute fiber content can create a congested structure that makes it harder to compact the geopolymer concrete properly, further weakening the matrix and leading to lower splitting tensile strength performance.

3.3.4. Flexural Strength

Figure 13 shows the flexural strength values of reinforced geopolymer concrete containing various lengths and volumes of natural jute fibers. The FS of geopolymer specimens evaluated at the ages of 1 and 4 weeks increased as the curing ages increased for all of the tested concrete specimens. The flexural strength of the reinforced geopolymer concretes was significantly affected by the fiber length and volume fraction. The test results showed that as the fiber length and volume content increased, the performance slightly improved compared with the control specimen. However, increasing the fiber length and volume content to a very high amount in the geopolymer mixtures resulted in a significant drop in its strength properties and led to lower performance. At 7 days, including 0.10, 0.20, 0.30, and 0.40% of 15 mm fibers led to an increase in flexural values from 4.16 to 4.45, 4.71, 4.94, and 5.32 MPa; then, the value dropped to 5.08, 4.82, and 4.32 MPa as the volume increased to 0.50, 0.60, and 0.70%, respectively. Likewise, the specimens evaluated at 28 days showed a significant improvement when the fiber content increased from 0.1 to 0.40% wherein the corresponding values of FS enhanced from 5.94 to 7.46 MPa. However, further raising the content of fibers to 0.50, 0.60 and 0.70% resulted in the flexural strength decreasing to 7.08, 6.72, and 6.34 MPa, as shown in Figure 13a. At the curing age of one week (Figure 13b), the specimen with 25 mm fibers added in volume fractions from 0.10 to 0.40% had improved FS ranging from 4.16 to 5.47 MPa, respectively. However, increasing the volume percentage to 0.50, 0.60 and 0.70% resulted in a drop in the flexural strength to 5.13, 4.69 and 4.41 MPa. Similar outcomes were found at the curing age of 4 weeks for the specimens with fiber volume fractions in the range of 0.10 to 0.40%, wherein the corresponding FS increased from 5.94 to 7.67 MPa. In addition, the FS values dropped to 6.52 MPa when the volume fractions of fibers in the concrete increased from 0.40% to 0.70%. As presented in Figure 13c, the specimens prepared with 35 mm fibers in volume fractions of 0.10, 0.20, 0.30, 0.40, 0.50, 0.60, and 0.70% achieved flexural strength values of 4.21, 4.49, 4.82, 5.16, 4.67, 4.32, 4.18 MPa at 7 days of age and 6.32, 6.68, 6.91, 7.29, 6.76, 6.44, and 5.98 MPa at 28 days of age, respectively. It clearly can be seen from the analysis that volume fractions of fibers higher than >0.40% led to a significant drop in flexural strength. Overall, the optimal fiber length and volume were 25 mm and 0.40%, respectively, which significantly improved the flexural strength by 31.5 and 29.1% at 7 and 28 days compared to the control.

Numerous studies have demonstrated that jute fibers generally improve the flexural strength of concrete composites [91–93]. Kansagra and Raval [94] observed that adding jute fibers in specific quantities increased both the tensile and flexural strength of concrete. It is well established that the insertion of jute fibers into the concrete matrix can enhance their mechanical characteristics, depending on the changing volume contents and lengths of the fibers [92]. Zia and Ali [47] examined the strength properties of jute fiber-reinforced concrete with a fiber length of 50 mm and cement mass of 5%. About a 36% reduction in the CS and 21% reduction in the TS was reported after the addition of jute fibers of higher lengths and amounts compared to the plain concrete. This decrease in strength performance was mainly due to the incorporation of a large volume of jute fibers with low density, which improved the concrete's heterogeneity. Another factor could be the reduced cement content in the jute fiber-reinforced concrete, as the fibers were introduced into a mix design ratio analogous to the plain mix. Additionally, the inadequate densification of the jute fiber-incorporated mixes associated with the weak absorption of water by the fibers could led to a reduced slump of the fresh mix, contributing to the decrease in the composite's strength [94].

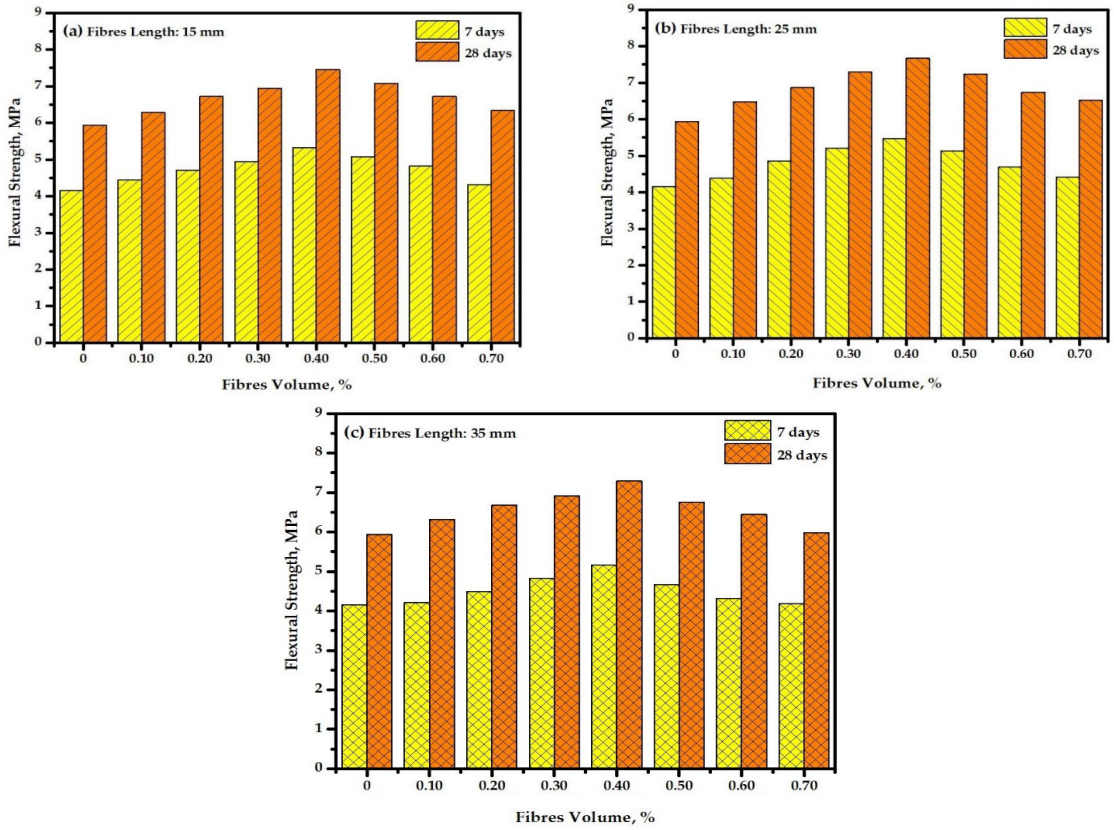

Figure 13. Effects of fiber length and content on flexural strength of proposed reinforced geopolymer concretes: (**a**) 15 mm, (**b**) 25 mm, (**c**) 35 mm.

The FS values of the fiber-reinforced geopolymer concretes were strongly interrelated with their STS, as shown in Figure 14. The STS values served as an indicator of the response factor and can be considered a predictive parameter. The experimental results were analyzed using a linear regression method, as shown in Equation (2). The R^2 value for all composites was found to be 0.97, indicating a high level of confidence in the correlation.

$$Flexural\ strength, MPa = (1.4435 \times splitting\ tensile\ strength) - 1.2223 \quad (2)$$

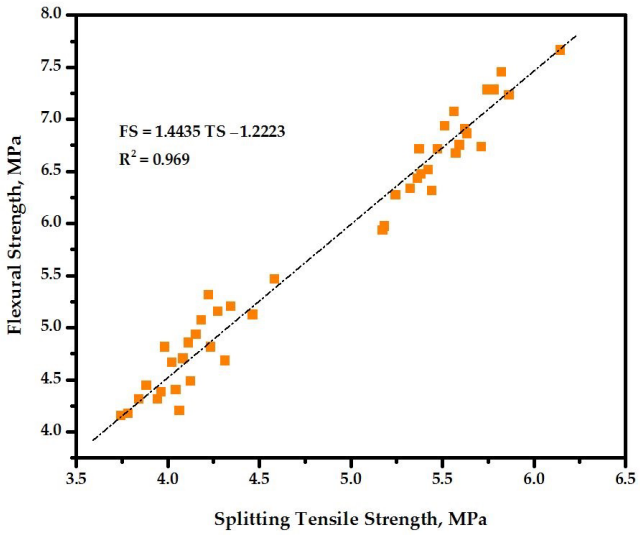

Figure 14. Relationship between splitting tensile strength and flexural strength of reinforced geopolymer concretes.

3.3.5. Elastic Modulus (MOE) of Concretes

The MOE values of the reinforced geopolymer concretes were also influenced by the fiber length and volume added to the matrix, which slightly dropped as the fiber lengths and volume fractions in the matrix increased. As shown in Figure 15, all the cylindrical concrete specimens made with different lengths and volume fractions of fibers displayed modulus of elasticity values lower than the control specimens. For reinforced geopolymer concrete specimens prepared with 15 mm fibers, increasing the fiber volume fractions from 0.10 to 0.70% led to a decrease in the corresponding values of MOE from 27.6 to 24.5 GPa compared to the control specimens (27.9 GPa) made without fiber reinforcement. Similarly, as the fiber length increased from 15 to 25 mm, the corresponding MOE values dropped from 27.6 to 27.4 GPa. Thereafter, the modulus decreased from 25.8 to 24.3 GPa with the corresponding increase in fiber volume content from 0.10 to 0.70%. Likewise, increasing the length of fibers from 15 and 25 mm to 35 mm resulted in a drop in the modulus to 27.1 GPa. Compared to control specimens, increasing the volume content of 35 mm fibers from 0% to 0.10%, 0.40% and 0.70% led to a significant decrease in the modulus from 27.9 to 27.1, 25.3, and 23.6 GPa, respectively. Various studies indicated that a higher volume fraction and length of fibers can lead to more voids and lower bond strength between the geopolymer pastes, aggregates and fibers, which resulted in a lower compressive strength and modulus of elasticity performance [69,95].

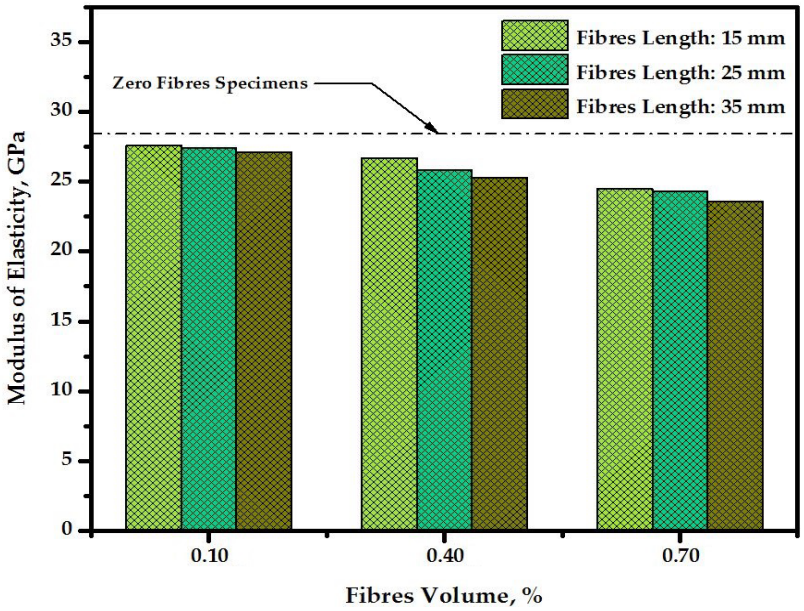

Figure 15. Modulus of elasticity of proposed geopolymer concretes.

There was a relationship between the MOE and CS of the reinforced geopolymer concrete specimens (Figure 16) in which the MOE values decreased as the CS of the geopolymer composites decreased. The experimentally obtained data were correlated by applying the linear regression approach via Equation (3), wherein the achieved R^2 value of 0.94 indicated a good correlation confidence.

$$Modulus\ of\ elasticity, GPa = (0.2858 \times compressive\ strength) + 14.499 \quad (3)$$

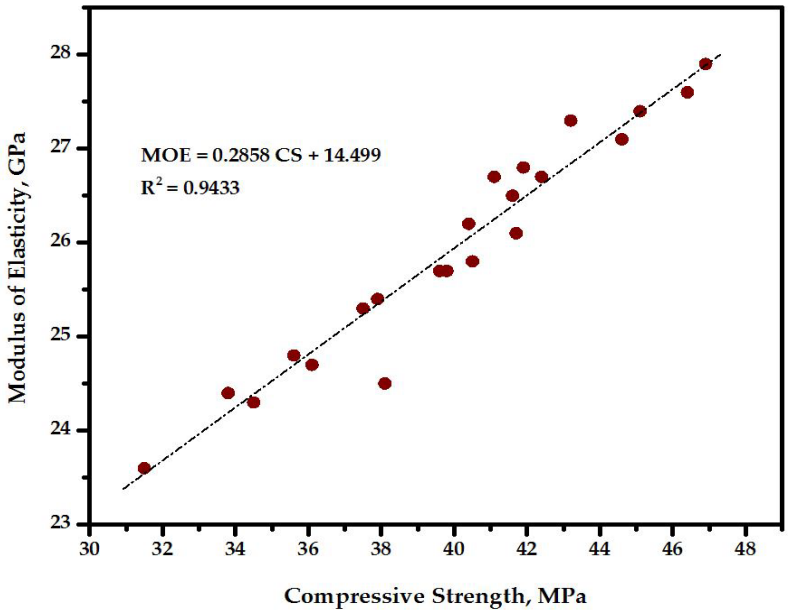

Figure 16. Relationship between the CS and MOE of the produced geopolymer concretes.

3.4. Water Absorption Capacity (WAC) of Concrete

Figure 17 illustrates the impact of the length and volume fractions of the reinforced fibers in the proposed geopolymer concretes on the WAC (after 4 weeks of curing age). The WAC of the concrete was directly correlated to the changing lengths and contents of the jute fibers. The results showed that increasing the fiber length from 15 to 35 mm and volume from 0.10% to 0.70% led to a significant increase in the WAC values. Figure 17a shows the effect of varying the volume (0.10% to 0.70%) of 15 mm fibers. Increasing the volume of fibers from 0% to 0.10, 0.20, 0.30, 0.40, 0.50, 0.60 and 0.70% resulted in an increase in the WAC from 3.87% to 3.95, 4.12, 4.24, 4.38, 4.56, 4.67, and 4.81%, respectively. When the fiber length was 25 mm (Figure 17b), a similar trend was observed: the WAC increased to 4.02, 4.17, 4.46, 4.64, 4.82, 4.94, and 5.06%, respectively. Likewise, and as shown in Figure 17c, increasing the fiber length to 35 mm increased the WAC values to 3.98, 4.23, 4.51, 4.74, 4.91, 5.08, and 5.24%, respectively. From the presented results, it clearly can be seen that the specimens prepared with longer fibers (35 mm) but similar volume percentages resulted in higher WAC values compared to the specimens prepared with 15 and 25 mm fibers. These results clearly demonstrated the strong influence of the fiber volume fractions and length on the porosity of the concrete matrix, wherein the matrix developed more pores when fibers with higher volume fractions and extended lengths were added into the concrete. This can be ascribed to the greater entrapment of air voids occurring after the fibers were introduced into the fresh mixes [96]. As a result, these air voids kept on increasing as the fiber volume fractions and length in the concrete matrix increased. Some reports suggested similar results for geopolymer composites made with other natural fibers, such as sugarcane bagasse fibers [97] and flax fibers [98], wherein with the increase in the fiber volume content, the WAC and porosity of the matrix also improved.

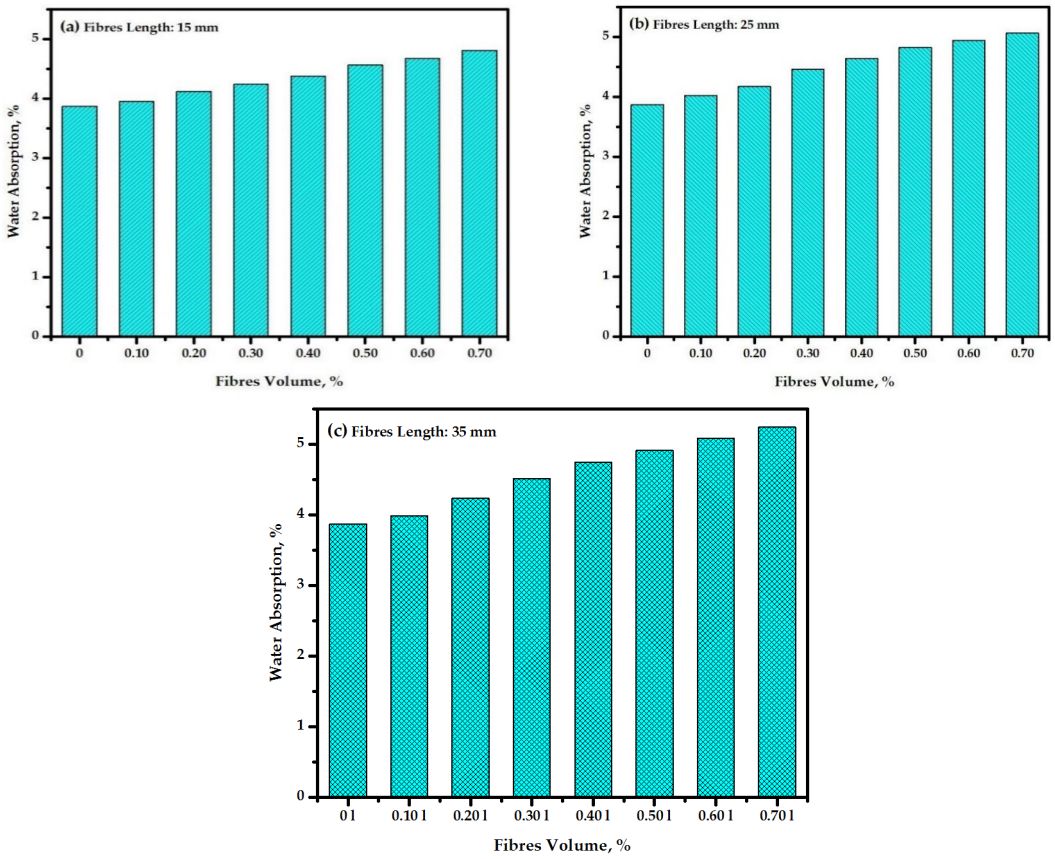

Figure 17. Effects of various lengths and volume fractions of fibers on the WAC of concretes, (**a**) 15 mm (**b**) 25 mm and (**c**) 35 mm.

As shown in Figure 18, there is an inverse relationship between the WAC and CS values of reinforced geopolymer concrete specimens. Water absorption tends to decrease as the compressive strength of the specimens increases. Once again, the experimentally obtained results were correlated using a linear regression approach, as expressed in Equation (4). The resulting R^2 value of 0.95 indicates a high level of confidence in the correlation.

$$Water\ absorption, \% = (-0.097 \times compressive\ strength) + 8.3974 \quad (4)$$

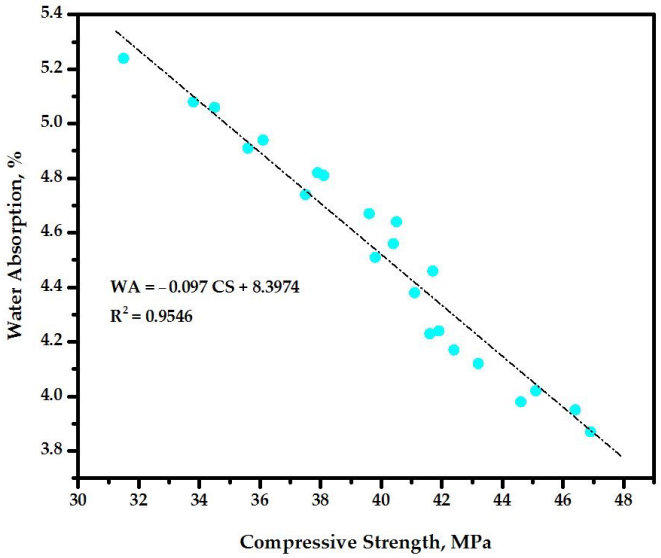

Figure 18. Correlation of CS and WAC of the studied concretes.

3.5. Microstructure Properties

3.5.1. X-Ray Diffraction (XRD) Analyses

The proposed geopolymer paste made of 75% of FA + 25% of GBFS was activated with a two-part alkaline solution, and the XRD profiles were recorded (Figure 19). Figure 19a displays the primary minerals of FA, revealing the existence of quartz, mullite, CaO, magnesium silicate, and aluminum–magnesium compounds. The diffraction patterns exhibited broad intense peaks in the 2-theta range of 20–30°, which is consistent with findings from previous studies [15,99], suggesting the presence of silica and alumina crystallites. However, the other pronounced diffraction peaks observed can be ascribed to the presence of quartz and mullite crystallites. In contrast, Figure 19b shows that GBFS particles do not exhibit sharp diffraction peaks, confirming their amorphous nature. A key factor in the formation of GBFS is its high content of reactive amorphous SiO_2 and CaO, which indicate its potential regarding geopolymer production. However, the addition of GBFS is necessary to compensate for the low calcium oxide content in FA, improving the geopolymerization process, reducing the setting times, and increasing the CS development at early and late ages. As presented in Figure 19c, the incorporated FA and GBFS together with the activation of a two-part alkali solution (6 M) led to a significant change in the chemical composition and decrease in the intensity of the peaks. More dense gels such as calcite ($CaCO_3$), albite ($Na(AlSi_3O_8)$), gismondine ($CaAl_2Si_2O_8 \cdot 4H_2O$), and muscovite ($KAl_2(Si_3Al)O_{10}(OH)_2$) appeared. These dense gels alongside the Na, Ca-(Al)-Si-H gels were created in response to the high early compressive strength of the proposed geopolymer concretes.

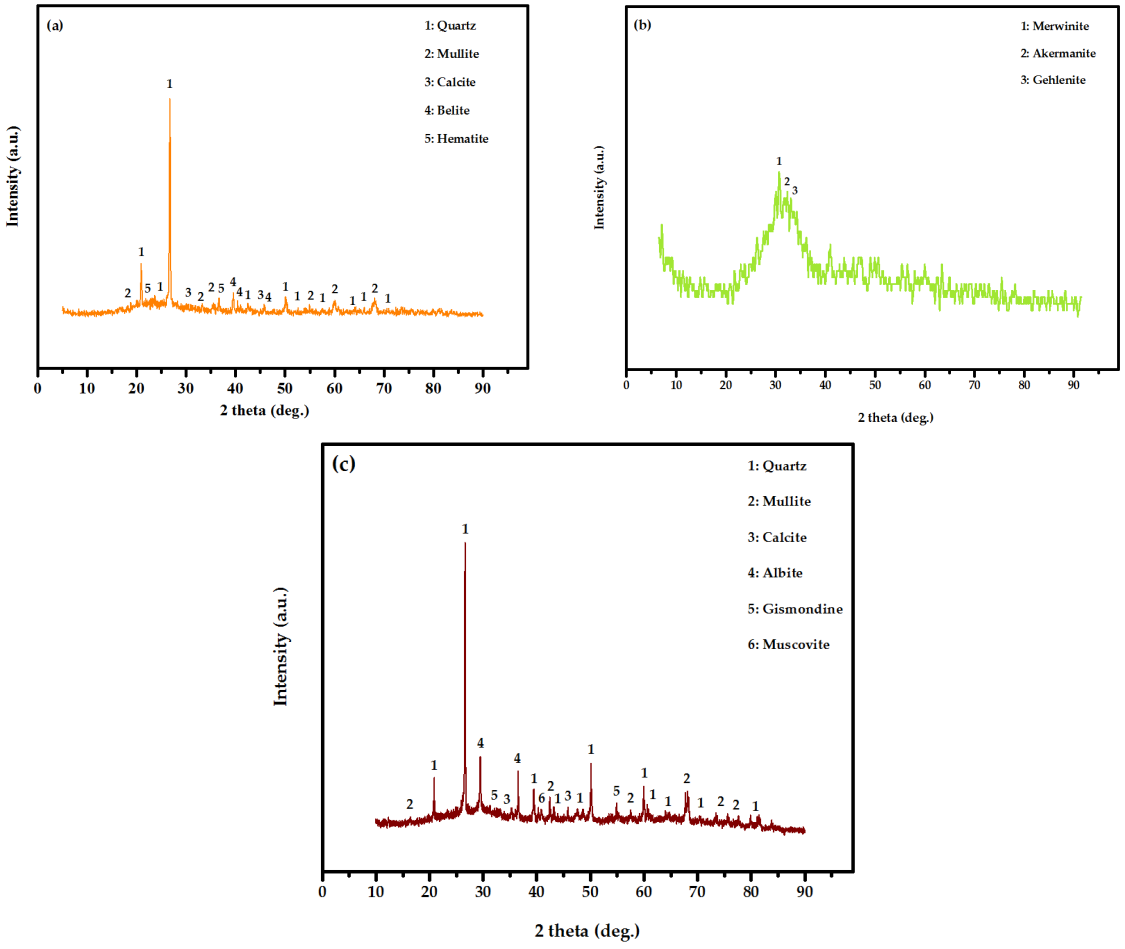

Figure 19. XRD profiles of (**a**) raw FA, (**b**) raw GBFS, and (**c**) geopolymer paste prepared with FA:GBFS of 75:25 and activated with two-part alkaline activator solution.

3.5.2. Scanning Electronic Microscopy (SEM) Analysis of Concretes

Figure 20 shows the SEM image analysis of FA, GBFS and geopolymers activated with alkaline activator solution. The surface morphologies of FA revealed the distribution of spherical particles (hollow) with a median size of 10 µm. These particles often contain smaller ones within their internal structure, which imparts ball-bearing characteristics to the FA, reducing the energy required to mix with GBFS in the formation of geopolymer paste, mortar, and concrete. Mehta and Siddique [100] and Li et al. [101] also observed similar particles morphology in FA. The SEM micrograph of GBFS (Figure 20b) shows the existence of an irregular distribution of angular particles with the median size of 12.4 µm, which was consistent with the observation of Poloju et al. [102]. The alkali solution activation of FA and GBFS dissolved the existing aluminosilicate and reacted with the calcium and sodium, formulating more dense gels and showing high early and late compressive strength. However, when the FA volume was high, more unreacted particles of FA were observed (Figure 20c).

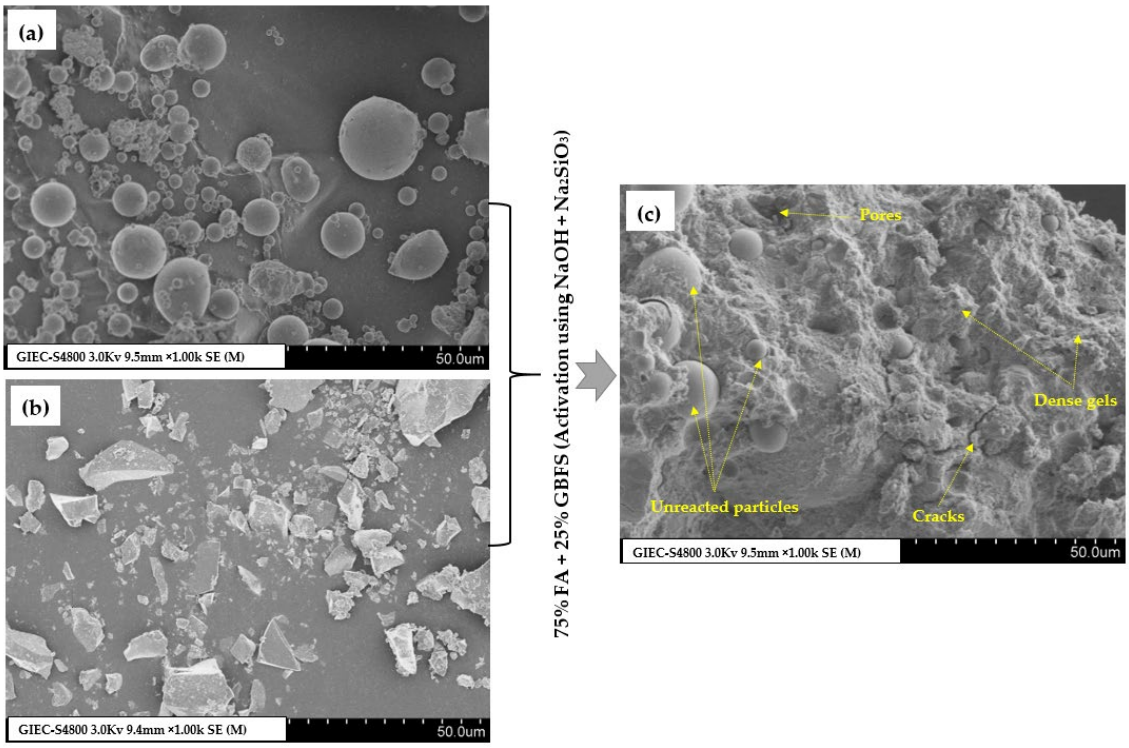

Figure 20. SEM micrographs of (**a**) raw FA, (**b**) raw GBFS, and (**c**) geopolymer concrete prepared with FA:GBFS of 75:25 activated with alkaline activator solution.

The surface morphology of jute fiber-reinforced geopolymer concretes with varying fiber length and volume is illustrated in Figure 21. The fiber length of 25 mm and volume of 0.40% (Figure 21b) was selected as the optimum addition due to the superior tensile and flexural strengths and surface morphology of the reinforced geopolymer concretes compared to those with a low (15 mm/0.10%) and high (35 mm/0.70%) fiber content, as shown in Figure 21a and c, respectively. At 100 µm magnification, it is evident that when the volume of jute fibers is high (Figure 21c), pores propagate into larger pores, and there are more voids between the fibers. When the fiber content is low, many micro-cracks were observed. However, in 0.40% jute fiber-reinforced geopolymers, there are fewer micro-cracks, indicating that jute fibers plays a role in inhibiting crack development. The figure also highlights fiber pull-out sites, which indicate a strong bond between the fibers and the matrix. Fiber pull-out, as opposed to fiber rupture, is desirable for enhancing the ductility of reinforced composites. A strong fiber–matrix bond was vital to prevent the breakage of fibers, enhancing the micro-cracking and ductility of concrete. This effective interaction

between the fibers and concrete matrix could enhance the absorption of energy such as fibers pull-out, de-bonding, and stress transferring from the concrete matrix to the fibers, explaining the observed STS and FS enhancement of the proposed geopolymers.

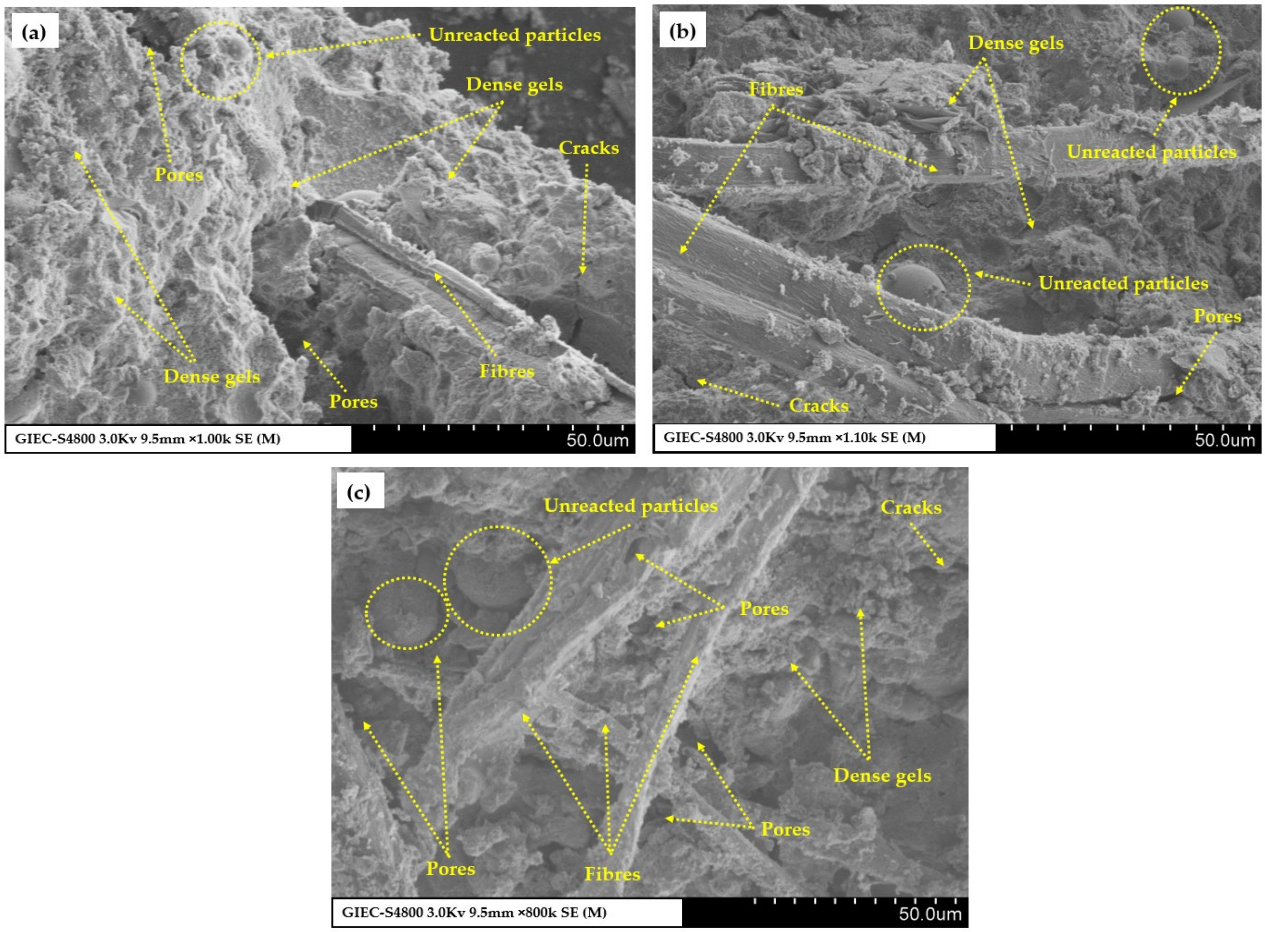

Figure 21. SEM micrographs of concrete prepared with jute natural fibers with a length–volume% of (**a**) 15 mm—0.10%, (**b**) 25 mm—0.40%, and (**c**) 35 mm—0.70%.

The surface morphology images further reveal the presence of unreacted FA particles when the fiber content was low, medium and high. However, the incorporation of jute fibers increased the formation of air voids around the fibers within the concrete matrix, thus reducing the geopolymers' workability. These findings are consistent with the lower density, compressive strength, and higher water absorption compared to the control specimens. To assess the influence of various volume fractions and lengths of fibers on the bonding strength of concrete, the SEM surface morphology of the mixes was analyzed. Figure 21a,b display the generation of strong bonds between the jute fibers and the composite network. However, in composites with 0.70% 35 mm jute fibers, loose bonding is observed at certain points (Figure 21c), which could hinder the stress transfer between the composite matrix and fibers, producing weak coupling amid the fibers and the composite matrix and reducing its strength performance. Compared to the bonds shown in Figure 21a,b, the jute fiber-reinforced geopolymers made with a volume fraction of 0.70% showed poor bonding between the jute fibers and composite matrix, which may be due to the poor distribution of fibers within the network resulting in more empty spaces and air voids. As the fiber volume fraction in the composite increased, the extent of matrix adjacent to each fiber was decreased, thereby weakening the fiber–matrix bond. Also, the SEM images of concrete showed that at longer fiber length and higher content, more air voids and pockets as well as macro-voids were formed around each fiber. When the proposed geopolymers are

subjected to external loads, these voids connect easily, causing failure in the geopolymer and breaking the matrix into small fragments, leading to a lower compressive strength performance. Regarding fiber length, the SEM images exhibited stronger bonding between the shorter fibers (15 and 25 mm) and composite matrix than for the longer fibers (35 mm). Geopolymers made with fiber lengths of 15 or 25 mm demonstrated the formation of strong bonds between the fibers and the composite matrix. However, some de-bonding was observed for specimens made with 15 mm fibers, which can be due to the reduced stress transfer to the fibers and lower tensile and flexural strengths. In contrast, geopolymers made with 35 mm fibers exhibited weaker adhesion between the fibers and composite matrix, displaying larger gaps, voids and air pockets around the region of the fibers and composite matrix. When the composites were subjected to load, these gaps expand and create voids, weakening the bond and resulting in failure at lower strengths compared to composites with 15 mm and 25 mm fibers.

3.5.3. Differential Thermogravimetry (TGA-DTG) Analyses

Figure 22 shows the TGA-DTG results of raw FA, raw GBFS and geopolymer composites prepared with a FA:GBFS ratio of 75:25. The weight changes occurred at different temperatures. The TGA results revealed a higher stability of FA at high temperature exposure than other specimens. In addition, the FA revealed drying (rerun) and desorption phases together with lower weight loss (1.27%). For the GBFS, a decomposition of multiphase without the formation of any intermediate products or faster rate of heating was seen wherein the weight loss was 2.31%. DTG data revealed the mass loss for the composites pre-set heating, suggesting a physical alteration of the raw materials. It was observed that the stability of the FA was higher, indicating its higher strength performance against any decomposition. FA also showed lower weight loss (0.0078%/°C) than GBFS because the decomposition peak of FA appeared after 700 °C. The TGA results confirmed a maximum change in weight for GBFS (0.02%/°C) at 718 °C. The results presented in Figure 22c show a significant change in the chemical composition of FA after it is mixed with GBFS and activated with an alkaline activator solution. More gels were formed, and the stability of Ca-OH and Ca-C-O bonds under heating was high with a weight loss of no more than 10.8% at 900 °C.

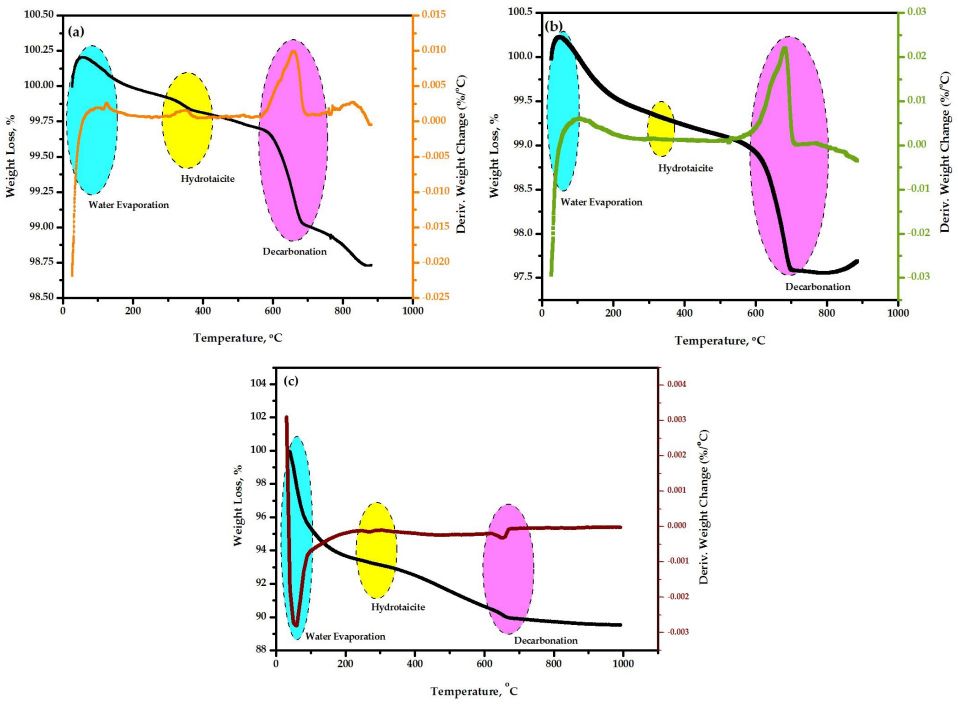

Figure 22. TGA-DTG analysis of (**a**) raw FA, (**b**) raw GBFS, and (**c**) geopolymer concrete prepared with FA:GBFS of 75:25.

3.5.4. Fourier-Transform Infrared Spectroscopy (FTIR) Analyses

FTIR measurement provided a deep insight into the vibrational signatures of chemical bonds in the constituent materials, enabling a thorough knowledge on the structural and chemical bonding properties The obtained crystalline to amorphous phase conversion of FA, GBFS, and geopolymer paste in the binary composite activated with alkali solution (after 28 days of age) under increasing temperatures was evaluated using FTIR spectral analyses. The stretching vibration modes depended on the Si–Al configuration in the structure, shifting toward lower wavenumbers with the increase in tetrahedral Al atoms [103]. Sitarz and Handke [104] observed broad absorption bands around 500–650 cm^{-1}, confirming the existence of silicate and aluminosilicate amorphous phase. These glassy phases exhibited a short-ranged order due to the presence of tetrahedral or octahedral ring-like structures. The band at 460 cm^{-1} was attributed to Al–O–Al in-plane bending vibration modes, while the band at 730 cm^{-1} emerged from the octahedral Al site vibration modes. The band at 820 cm^{-1} was originated from stretching vibration modes of tetrahedral Al–O [105]. The band at 1400 cm^{-1} was due to asymmetric stretching vibration modes of Al–O/Si–O linkages [106]. Raw FA (Figure 23a) displayed a broad band with intermediate intensity (C–O/C=O) around 1460 to 1600 cm^{-1}. In contrast, GBFS (Figure 23b) exhibited higher vibrational modes. Both FA and GBFS showed broad bands around 3500 cm^{-1}, which was due to the bending vibration modes of (C=O–H) and stretching vibration modes of hydroxyl group (–OH), indicating the presence of weakly bonded water molecules adsorbed or trapped on the materials surface or in large voids. In Figure 23c, the analysis results showed a significant change in the chemical composition, and more silica and aluminum dissolved and dense gels formulated.

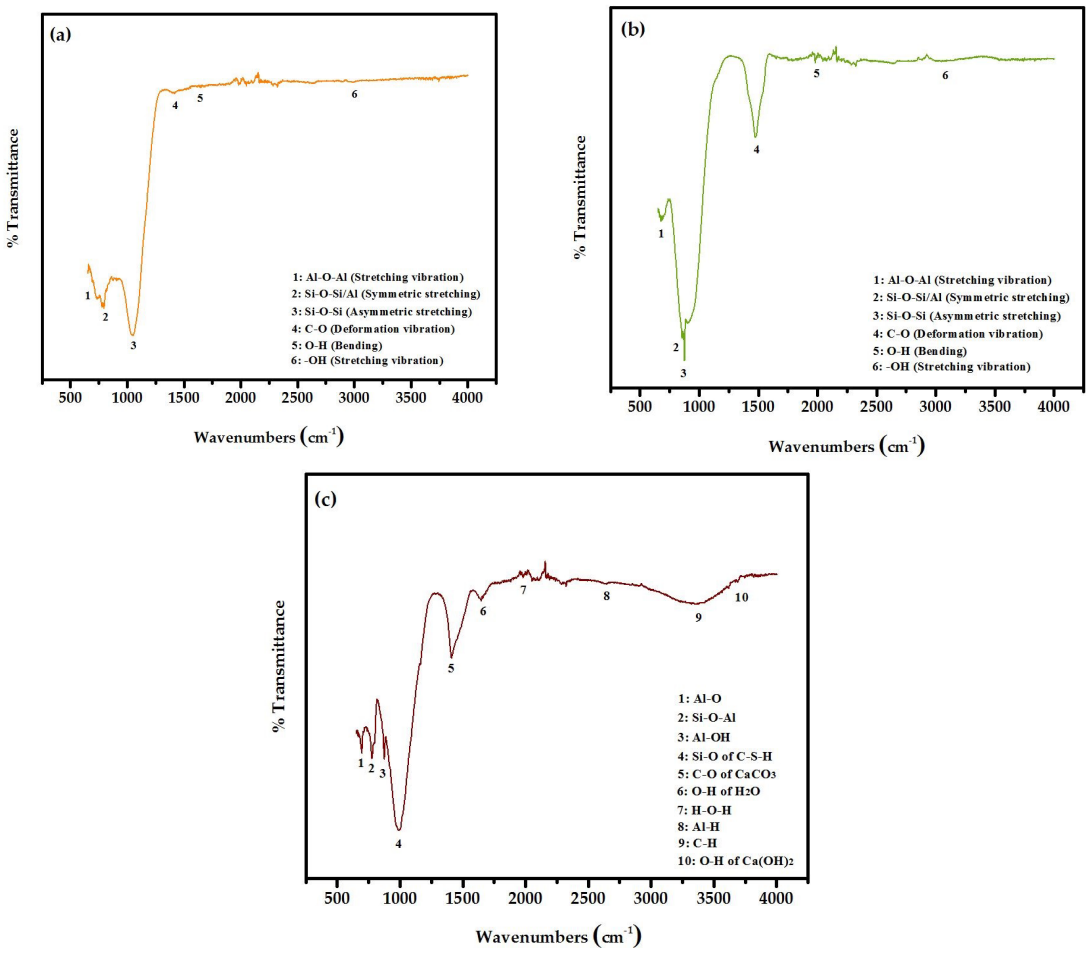

Figure 23. FTIR spectrum of (**a**) raw FA, (**b**) raw GBFS, and (**c**) geopolymer concrete prepared with an FA:GBFS ratio of 75:25.

4. Applications, Opportunities, and Prospects

The applications, opportunities, and prospects of natural jute fibers in geopolymer concrete technology are significant due to their sustainability, cost effectiveness, and environmental benefits.

There are several potential applications for jute fibers in the geopolymer concrete industry. (i) Reinforcement in Concrete: Natural jute fibers are used to reinforce concrete, improving its tensile strength, flexural strength, and toughness, as shown in Figure 24. (ii) Lightweight Concrete: These fibers help produce lightweight concrete, which is ideal for non-structural components, reducing the overall load on structures. (iii) Crack Control: Jute fibers are effective in controlling shrinkage cracks in concrete, enhancing the durability and service life of structures. (iv) Precast Concrete Elements: Natural fibers are also used in precast concrete products such as blocks, panels, and roofing tiles, offering eco-friendly alternatives to traditional materials.

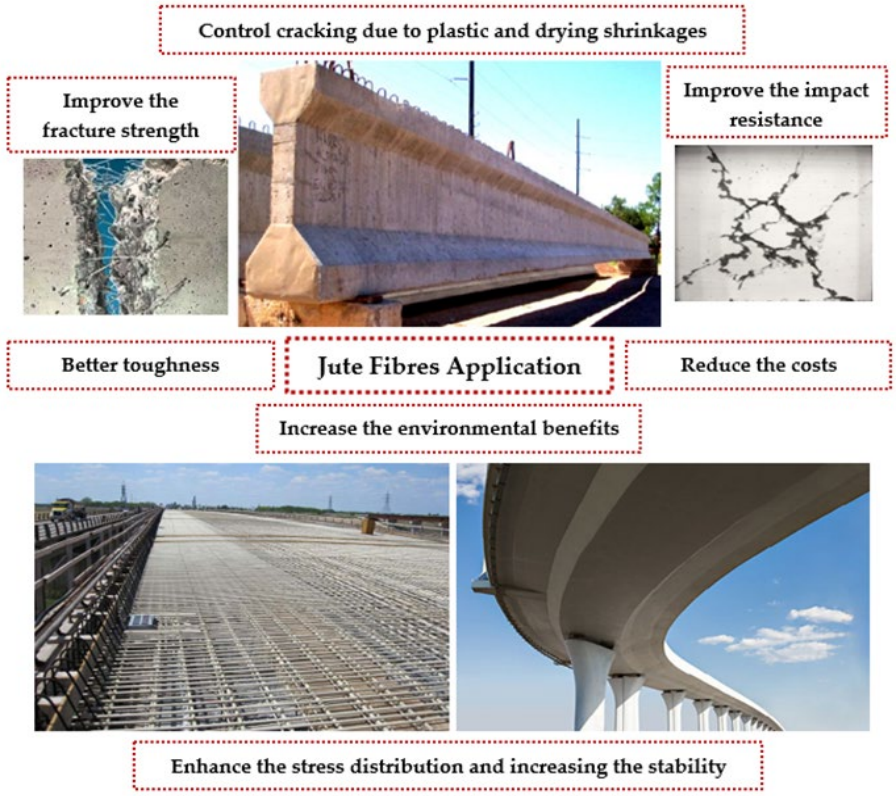

Figure 24. Potential applications of jute fibers in geopolymer concrete industry.

Jute fibers present several eco-friendly opportunities. (i) Sustainable Construction: Natural fibers provide a greener alternative to synthetic fibers and steel, reducing the carbon footprint of concrete production. (ii) Cost-Effective Solutions: Jute fibers offer a cost-effective reinforcement option, especially in regions where natural fibers are abundant and affordable. (iii) Waste Utilization: The use of agricultural by-products (such as straw or hemp fibers) as reinforcement materials in concrete creates opportunities for recycling waste materials. (iv) Innovation in Materials: The development of hybrid composites, combining natural and synthetic fibers, opens new possibilities for optimizing the mechanical properties of fiber-reinforced concrete.

As for future prospects, jute fibers have significant potential. (i) Wider Adoption in Green Building: With the growing emphasis on sustainable construction, natural fiber-reinforced concrete has strong potential for wider use in green building certifications and eco-friendly designs. (ii) Enhanced Performance through Research: Ongoing research into the treatment and modification of natural fibers to improve their bonding with the concrete matrix could lead to higher-performing materials. (iii) Regulatory Support: As

more countries implement regulations promoting sustainable construction, the use of natural fibers in concrete could become more standardized and widely accepted. (iv) Long-Term Durability: Continued advances in understanding the durability and degradation mechanisms of natural fibers in concrete will further encourage their adoption in long-lasting structures.

In summary, natural jute fibers in geopolymer concrete technology hold great promise for eco-friendly construction, and their applications will likely expand as research and technology continue to improve performance and durability.

5. Conclusions

In this study, the effect of incorporating natural jute fibers of varying lengths and volume fractions on the structures, morphologies, workability, thermal stabilities and engineering characteristics of fiber-reinforced geopolymer composites was evaluated. The proposed concrete specimens were prepared and analyzed using diverse tests. The test results of the obtained geopolymer concretes were compared with the control specimen (without jute fibers reinforcement). From the obtained results, the following conclusions were drawn:

i. Geopolymer concrete mixes were designed using a high volume of FA (75%) and GBFS (25%) followed by the activation using a two-part alkali solution made from NH and NS at 6 M molarity.
ii. Jute fibers with varying lengths (15 mm, 25 mm and 35 mm) and volume fractions (0.10, 0.20, 0.30, 0.40, 0.50, 0.60, and 0.70%) were used to prepare the reinforced geopolymer concretes.
iii. The workability of the reinforced geopolymer concrete was significantly influenced by the length and volume of the fibers. The slump values decreased with longer fiber lengths and higher volume fractions. The lowest slump was observed in a geopolymer mixture containing fibers that were 35 mm in length and 0.70% in volume. A direct correlation was identified between fiber volume and slump values.
iv. The CS values of fiber-reinforced specimens were slightly decreased as the fiber lengths and volume fractions increased in the geopolymer matrix. Compared to the control specimen' compressive strength (46.9 MPa), specimens prepared with volume 35 mm—0.70% achieved the lowest CS of 31.5 MPa at 4 weeks of curing age.
v. The inclusion of 0.10, 0.20, 0.30, and 0.40% jute fiber volume significantly enhanced the splitting tensile and flexural strength performance. However, increasing the jute fibers content up to 0.50% negatively affected the strength performance and led to lower strength values, more voids, weak bond with the geopolymer paste, and lower performance. Specimens prepared with a fiber length of 25 mm and volume fraction of 0.40% achieved the optimum fracture strength at early and late ages compared with the other mixtures of reinforced geopolymers. At 28 days of age, the optimum mixture achieved an increase of 18.7 and 29.1% in the corresponding STS and FS values.
vi. A strong relationship was observed between the CS and MOE for the achieved jute fiber-reinforced geopolymer specimens. Increasing the fiber length and volume content slightly led to a drop in the modulus values.
vii. The water absorption capacity of the proposed geopolymer concrete was significantly affected by the variation in the fiber volume fraction and length. When the fiber length increased from 15 to 35 mm and volume fraction increased from 0.10% to 0.70%, the WAC of concrete was enhanced and reached the highest percentage of 5.24%.
viii. The microstructure performance of the geopolymer concrete was assessed by XRD, FESEM, TGA-DTG, and FTIR. The results indicated significant changes in the chemical and mineral properties of binary blends of FA-GBFS after being activated with alkaline activator solution, which indicated the formation of denser gels, enhancing the early and late strength performance.
ix. The analysis results of surface morphology showed that the composites with higher fiber length and content (35 mm, 0.70%) have more air voids and pockets (both micro

and macro) adjacent to the fibers within the concrete matrix. When the proposed geopolymers were subjected to external loads, these voids connected easily, causing failure in the geopolymer, breaking the matrix into small fragments and leading to lower compressive strength performance.

6. Recommendation for Future Investigation

Further studies are essential for obtaining adequate information on the effectiveness of jute fiber-reinforced geopolymer concrete as a high performance eco-friendly construction material. (i) The effect of different types of binders, alkaline activator solution molarity and modulus, curing regime and ratio of solution to binder and binder to filler on the workability and strength performance of jute fibers reinforced geopolymer concretes deserves further study. (ii) The effect of the jute fibers' length and volume on plastic and drying shrinkage of the proposed geopolymer concrete needs further investigation. (iii) The durability performance of geopolymer concrete prepared with jute fibers of varying length and volume in aggressive environments such as sulfuric acid, sulfate, elevated temperatures, freeze–thaw and wet–dry cycles is yet to be analyzed. (iv) The thermal and acoustic properties of jute fiber-based geopolymer concrete require analysis. (v) Jute fiber-based hybrid fibers for ultra-high strength geopolymer concrete need further study. (vi) Last, the environmental benefits and life cycle assessment of jute fiber-reinforced geopolymer concretes also need to be evaluated.

Author Contributions: Conceptualization, A.D.A.A.M. and W.R.; methodology, A.D.A.A.M.; software, G.F.H.; validation, A.D.A.A.M., W.R. and G.F.H.; formal analysis, A.D.A.A.M.; investigation, A.D.A.A.M.; resources A.D.A.A.M.; data curation, A.D.A.A.M.; writing—original draft preparation, A.D.A.A.M.; writing—review and editing, W.R. and G.F.H.; visualization, W.R.; supervision, W.R.; project administration, G.F.H.; funding acquisition, A.D.A.A.M. and G.F.H. All authors have read and agreed to the published version of the manuscript.

Funding: This research received no external funding.

Data Availability Statement: Data are contained within the article.

Acknowledgments: The authors thank South China University of Technology for their support and cooperation to conduct this research.

Conflicts of Interest: The authors declare no conflicts of interest.

References

1. Rihan, M.A.M.; Onchiri, R.O.; Gathimba, N.; Sabuni, B. Assessing the Durability Performance of Geopolymer Concrete Utilizing Fly Ash and Sugarcane Bagasse Ash as Sustainable Binders. *Open Ceram.* **2024**, *20*, 100687. [CrossRef]
2. Maradani, L.S.R.; Pradhan, B. Effect of chloride and sulphate on ionic concentration of aqueous pore solution and microstructural properties of fly ash-GBFS geopolymer concrete. *Constr. Build. Mater.* **2024**, *440*, 137422. [CrossRef]
3. Ariyadasa, P.W.; Manalo, A.C.; Lokuge, W.; Aravinthan, V.; Pasupathy, K.; Gerdes, A. Bond performance of fly ash-based geopolymer mortar in simulated concrete sewer substrate. *Constr. Build. Mater.* **2024**, *446*, 137927. [CrossRef]
4. Huseien, G.F.; Sam, A.R.M.; Alyousef, R. Texture, morphology and strength performance of self-compacting alkali-activated concrete: Role of fly ash as GBFS replacement. *Constr. Build. Mater.* **2021**, *270*, 121368. [CrossRef]
5. Huseien, G.F.; Ismail, M.; Tahir, M.M.; Mirza, J.; Khalid, N.H.A.; Asaad, M.A.; Husein, A.A.; Sarbini, N.N. Synergism between palm oil fuel ash and slag: Production of environmental-friendly alkali activated mortars with enhanced properties. *Constr. Build. Mater.* **2018**, *170*, 235–244. [CrossRef]
6. Chanda, S.S.; Guchhait, S. A comprehensive review on the factors influencing engineering characteristics of lightweight geopolymer concrete. *J. Build. Eng.* **2024**, *86*, 108887. [CrossRef]
7. Zhao, C.; Li, Z.; Peng, S.; Liu, J.; Wu, Q.; Xu, X. State-of-the-Art Review of Geopolymer Concrete Carbonation: From Impact Analysis to Model Establishment. *Case Stud. Constr. Mater.* **2024**, *20*, e03124. [CrossRef]
8. Shaikh, N.D.; Shah, N.D. Advancements in self-compacting geopolymer concrete: A comprehensive overview. *Mater. Today Proc.* **2023**, *93*, 545–551. [CrossRef]
9. Luo, Y.; Yang, L.; Wang, D.; Zhang, Q.; Wang, Z.; Xing, M.; Xue, G.; Zhang, J.; Liu, Z. Effect of GGBFS on the mechanical properties of metakaolin-based self-compacting geopolymer concrete. *J. Build. Eng.* **2024**, *96*, 110501. [CrossRef]
10. Huseien, G.F.; Mirza, J.; Ismail, M.; Hussin, M.W. Influence of different curing temperatures and alkali activators on properties of GBFS geopolymer mortars containing fly ash and palm-oil fuel ash. *Constr. Build. Mater.* **2016**, *125*, 1229–1240. [CrossRef]

11. Huseien, G.F.; Mirza, J.; Ismail, M.; Ghoshal, S.; Ariffin, M.A.M. Effect of metakaolin replaced granulated blast furnace slag on fresh and early strength properties of geopolymer mortar. *Ain Shams Eng. J.* **2018**, *9*, 1557–1566. [CrossRef]
12. Ahmat, A.M.; Alengaram, U.J.; Shamsudin, M.F.; Alnahhal, A.M.; Ibrahim, M.S.I.; Ibrahim, S.; Rashid, R. Assessment of sustainable eco-processed pozzolan (EPP) from palm oil industry as a fly ash replacement in geopolymer concrete. *Constr. Build. Mater.* **2023**, *387*, 131424. [CrossRef]
13. Tanu, H.; Unnikrishnan, S. Review on durability of geopolymer concrete developed with industrial and agricultural byproducts. *Mater. Today Proc.* **2023**, *94*, 1–7. [CrossRef]
14. Mohd Ariffin, M.A.; Hussin, M.W.; Rafique Bhutta, M.A. Mix design and compressive strength of geopolymer concrete containing blended ash from agro-industrial wastes. *Adv. Mater. Res.* **2011**, *339*, 452–457. [CrossRef]
15. Huseien, G.F.; Sam, A.R.M.; Shah, K.W.; Mirza, J.; Tahir, M.M. Evaluation of alkali-activated mortars containing high volume waste ceramic powder and fly ash replacing GBFS. *Constr. Build. Mater.* **2019**, *210*, 78–92. [CrossRef]
16. Ansari, M.A.; Shariq, M.; Mahdi, F. Geopolymer concrete for clean and sustainable construction–A state-of-the-art review on the mix design approaches. *Structures* **2023**, *55*, 1045–1070. [CrossRef]
17. Yang, X.; Wu, S.; Xu, S.; Chen, B.; Chen, D.; Wang, F.; Jiang, J.; Fan, L.; Tu, L. Effects of GBFS content and curing methods on the working performance and microstructure of ternary geopolymers based on high-content steel slag. *Constr. Build. Mater.* **2024**, *410*, 134128. [CrossRef]
18. Zhang, D.; Zhu, H.; Wu, Q.; Yang, T.; Yin, Z.; Tian, L. Investigation of the hydrophobicity and microstructure of fly ash-slag geopolymer modified by polydimethylsiloxane. *Constr. Build. Mater.* **2023**, *369*, 130540. [CrossRef]
19. Nassar, A.K.; Kathirvel, P. Effective utilization of agricultural waste in synthesizing activator for sustainable geopolymer technology. *Constr. Build. Mater.* **2023**, *362*, 129681. [CrossRef]
20. Pradhan, P.; Dwibedy, S.; Pradhan, M.; Panda, S.; Panigrahi, S.K. Durability characteristics of geopolymer concrete-Progress and perspectives. *J. Build. Eng.* **2022**, *59*, 105100. [CrossRef]
21. Uysal, M.; Kuranlı, Ö.F.; Aygörmez, Y.; Canpolat, O.; Çoşgun, T. The effect of various fibers on the red mud additive sustainable geopolymer composites. *Constr. Build. Mater.* **2023**, *363*, 129864. [CrossRef]
22. Teng, S.; Afroughsabet, V.; Ostertag, C.P. Flexural behavior and durability properties of high performance hybrid-fiber-reinforced concrete. *Constr. Build. Mater.* **2018**, *182*, 504–515. [CrossRef]
23. Kaplan, G.; Coskan, U.; Benli, A.; Bayraktar, O.Y.; Kucukbaltacı, A.B. The impact of natural and calcined zeolites on the mechanical and durability characteristics of glass fiber reinforced cement composites. *Constr. Build. Mater.* **2021**, *311*, 125336. [CrossRef]
24. Xu, Z.; Liu, Q.; Long, H.; Deng, H.; Chen, Z.; Hui, D. Influence of nano-SiO_2 and steel fiber on mechanical and microstructural properties of red mud-based geopolymer concrete. *Constr. Build. Mater.* **2023**, *364*, 129990. [CrossRef]
25. Li, J.; Si, J.; Luo, F.; Zuo, C.; Zhang, P.; Sun, Y.; Li, W.; Miao, S. Self-compensating geopolymer utilizing nano-clay and chopped basalt fibers. *Constr. Build. Mater.* **2022**, *357*, 129302. [CrossRef]
26. Farhan, K.Z.; Johari, M.A.M.; Demirboğa, R. Impact of fiber reinforcements on properties of geopolymer composites: A review. *J. Build. Eng.* **2021**, *44*, 102628. [CrossRef]
27. Akarken, G.; Cengiz, U. Fabrication and characterization of metakaolin-based fiber reinforced fire resistant geopolymer. *Appl. Clay Sci.* **2023**, *232*, 106786. [CrossRef]
28. Zhao, J.; Trindade, A.C.C.; Liebscher, M.; de Andrade Silva, F.; Mechtcherine, V. A review of the role of elevated temperatures on the mechanical properties of fiber-reinforced geopolymer (FRG) composites. *Cem. Concr. Compos.* **2023**, *137*, 104885. [CrossRef]
29. Yan, S.; He, P.; Jia, D.; Yang, Z.; Duan, X.; Wang, S.; Zhou, Y. Effect of fiber content on the microstructure and mechanical properties of carbon fiber felt reinforced geopolymer composites. *Ceram. Int.* **2016**, *42*, 7837–7843. [CrossRef]
30. Ganesan, N.; Abraham, R.; Raj, S.D. Durability characteristics of steel fibre reinforced geopolymer concrete. *Constr. Build. Mater.* **2015**, *93*, 471–476. [CrossRef]
31. Su, Z.; Guo, L.; Zhang, Z.; Duan, P. Influence of different fibers on properties of thermal insulation composites based on geopolymer blended with glazed hollow bead. *Constr. Build. Mater.* **2019**, *203*, 525–540. [CrossRef]
32. Alzeebaree, R.; Çevik, A.; Nematollahi, B.; Sanjayan, J.; Mohammedameen, A.; Gülşan, M.E. Mechanical properties and durability of unconfined and confined geopolymer concrete with fiber reinforced polymers exposed to sulfuric acid. *Constr. Build. Mater.* **2019**, *215*, 1015–1032. [CrossRef]
33. Wongprachum, W.; Sappakittipakorn, M.; Sukontasukkul, P.; Chindaprasirt, P.; Banthia, N. Resistance to sulfate attack and underwater abrasion of fiber reinforced cement mortar. *Constr. Build. Mater.* **2018**, *189*, 686–694. [CrossRef]
34. Haily, E.; Zari, N.; Bouhfid, R.; Qaiss, A. Natural fibers as an alternative to synthetic fibers in the reinforcement of phosphate sludge-based geopolymer mortar. *J. Build. Eng.* **2023**, *67*, 105947. [CrossRef]
35. Wang, Y.; Huang, X.; Guo, S.; Zhang, X.; Nie, Y. An experimental investigation on freeze-thaw resistance of fiber-reinforced red mud-slag based geopolymer. *Case Stud. Constr. Mater.* **2024**, *20*, e03409. [CrossRef]
36. Gholampour, A.; Ozbakkaloglu, T. A review of natural fiber composites: Properties, modification and processing techniques, characterization, applications. *J. Mater. Sci.* **2020**, *55*, 829–892. [CrossRef]
37. Das, T.K.; Jesionek, M. Synthesis, Properties, and Characterization of Fibrous Filler. In *Fiber and Ceramic Filler-Based Polymer Composites for Biomedical Engineering*; Springer: Berlin/Heidelberg, Germany, 2024; pp. 63–85.
38. Gholampour, A.; Danish, A.; Ozbakkaloglu, T.; Yeon, J.H.; Gencel, O. Mechanical and durability properties of natural fiber-reinforced geopolymers containing lead smelter slag and waste glass sand. *Constr. Build. Mater.* **2022**, *352*, 129043. [CrossRef]

39. Bordoloi, S.; Ng, C. Feasibility of construction demolition waste for unexplored geotechnical and geo-environmental applications-a review. *Constr. Build. Mater.* **2022**, *356*, 129230.
40. Peng, C.-L.; Scorpio, D.E.; Kibert, C.J. Strategies for successful construction and demolition waste recycling operations. *Constr. Manag. Econ.* **1997**, *15*, 49–58. [CrossRef]
41. Ok, B.; Sarici, T.; Talaslioglu, T.; Yildiz, A. Geotechnical properties of recycled construction and demolition materials for filling applications. *Transp. Geotech.* **2020**, *24*, 100380. [CrossRef]
42. Wongsa, A.; Kunthawatwong, R.; Naenudon, S.; Sata, V.; Chindaprasirt, P. Natural fiber reinforced high calcium fly ash geopolymer mortar. *Constr. Build. Mater.* **2020**, *241*, 118143. [CrossRef]
43. Silva, G.; Kim, S.; Bertolotti, B.; Nakamatsu, J.; Aguilar, R. Optimization of a reinforced geopolymer composite using natural fibers and construction wastes. *Constr. Build. Mater.* **2020**, *258*, 119697. [CrossRef]
44. Mansur, M.; Aziz, M. A study of jute fibre reinforced cement composites. *Int. J. Cem. Compos. Lightweight Concr.* **1982**, *4*, 75–82. [CrossRef]
45. Kundu, S.P.; Chakraborty, S.; Roy, A.; Adhikari, B.; Majumder, S. Chemically modified jute fibre reinforced non-pressure (NP) concrete pipes with improved mechanical properties. *Constr. Build. Mater.* **2012**, *37*, 841–850. [CrossRef]
46. Saha, S.; Mohanty, T. Effects on jute fiber and ferrochrome slag as coarse aggregate on mechanical properties of reinforced concrete. *Mater. Today Proc.* **2023**, *92*, 1–7. [CrossRef]
47. Zia, A.; Ali, M. Behavior of fiber reinforced concrete for controlling the rate of cracking in canal-lining. *Constr. Build. Mater.* **2017**, *155*, 726–739. [CrossRef]
48. Hasan, R.; Sobuz, M.; Akid, A.; Awall, M.; Houda, M.; Saha, A.; Meraz, M.; Islam, M.; Sutan, N. Eco-friendly self-consolidating concrete production with reinforcing jute fiber. *J. Build. Eng.* **2023**, *63*, 105519. [CrossRef]
49. Islam, M.S.; Ahmed, S.J. Influence of jute fiber on concrete properties. *Constr. Build. Mater.* **2018**, *189*, 768–776. [CrossRef]
50. Zhang, T.; Yin, Y.; Gong, Y.; Wang, L. Mechanical properties of jute fiber-reinforced high-strength concrete. *Struct. Concr.* **2020**, *21*, 703–712. [CrossRef]
51. Ramnath, B.V.; Manickavasagam, V.; Elanchezhian, C.; Krishna, C.V.; Karthik, S.; Saravanan, K. Determination of mechanical properties of intra-layer abaca-jute-glass fiber reinforced composite. *Mater. Des.* **2014**, *60*, 643–652. [CrossRef]
52. Zakaria, M.; Ahmed, M.; Hoque, M.M.; Hannan, A. Effect of jute yarn on the mechanical behavior of concrete composites. *SpringerPlus* **2015**, *4*, 731. [CrossRef]
53. Kim, J.-s.; Lee, H.-j.; Choi, Y. Mechanical properties of natural fiber-reinforced normal strength and high-fluidity concretes. *Comput. Concr. Int. J.* **2013**, *11*, 531–539. [CrossRef]
54. Hamzah, H.K.; Huseien, G.F.; Asaad, M.A.; Georgescu, D.P.; Ghoshal, S.; Alrshoudi, F. Effect of waste glass bottles-derived nanopowder as slag replacement on mortars with alkali activation: Durability characteristics. *Case Stud. Constr. Mater.* **2021**, *15*, e00775. [CrossRef]
55. Lam, T.F.; bin Mohamad Yatim, J. Mechanical properties of kenaf fiber reinforced concrete with different fiber content and fiber length. *J. Asian Concr. Fed.* **2015**, *1*, 11–21. [CrossRef]
56. Mahzabin, M.S.; Hock, L.J.; Hossain, M.S.; Kang, L.S. The influence of addition of treated kenaf fibre in the production and properties of fibre reinforced foamed composite. *Constr. Build. Mater.* **2018**, *178*, 518–528. [CrossRef]
57. Ibrahim, M.I.; Hassan, M.Z.; Dolah, R.; Yusoff, M.Z.M.; Salit, M.S. Tensile behaviour for mercerization of single kenaf fiber. *Malays. J. Fundam. Appl. Sci* **2018**, *14*, 437–439. [CrossRef]
58. *ASTM C579*; Standard Test Methods for Compressive Strength of Chemical-Resistant Mortars, Grouts, Monolithic Surfacings and Polymer Concretes. ASTM International: West Conshohocken, PA, USA, 2001.
59. *ASTM C143*; Standard Test Method for Slump of Hydraulic-Cement Concrete. ASTM International: West Conshohocken, PA, USA, 2015.
60. *BS EN 12350-2*; Testing Fresh Concrete. Slump-Test. British Standards Publishing: London, UK, 2009.
61. *BS EN 12390-3*; Testing Hardened Concrete. Compressive Strength of Test Specimens. British Standards Publishing: London, UK, 2009.
62. *BS EN 12390-6*; Testing Hardened Concrete. Tensile Strength of Test Specimens. British Standards Publishing: London, UK, 2009.
63. *BS EN 12390-5*; Testing Hardened Concrete. Flexural Strength of Test Specimens. British Standards Publishing: London, UK, 2009.
64. *ASTM C469*; Standard Test Method for Static Modulus of Elasticity and Poisson's Ratio of Concrete in Compression. ASTM International: West Conshohocken, PA, USA, 2010.
65. *ASTM C642*; Standard Test Method for Density, Absorption, and Voids in Hardened Concrete. ASTM International: West Conshohocken, PA, USA, 2013.
66. Muhammad, A.; Rashidi, A.R.; Wahit, M.U.; Sanusi, S.N.A.; Iziuna, S.; Jamaludin, S. Alkaline treatment on kenaf fiber to be incorporated in unsaturated polyester. *J. Eng. Appl. Sci* **2016**, *11*, 11894–11897.
67. Saha, P.; Manna, S.; Chowdhury, S.R.; Sen, R.; Roy, D.; Adhikari, B. Enhancement of tensile strength of lignocellulosic jute fibers by alkali-steam treatment. *Bioresour. Technol.* **2010**, *101*, 3182–3187. [CrossRef]
68. Guo, A.; Sun, Z.; Satyavolu, J. Impact of chemical treatment on the physiochemical and mechanical properties of kenaf fibers. *Ind. Crops Prod.* **2019**, *141*, 111726. [CrossRef]
69. Song, H.; Liu, J.; He, K.; Ahmad, W. A comprehensive overview of jute fiber reinforced cementitious composites. *Case Stud. Constr. Mater.* **2021**, *15*, e00724. [CrossRef]

70. Nwankwo, C.O.; Mahachi, J.; Olukanni, D.O.; Musonda, I. Natural fibres and biopolymers in FRP composites for strengthening concrete structures: A mixed review. *Constr. Build. Mater.* **2023**, *363*, 129661. [CrossRef]
71. Abbas, A.G.N.; Aziz, F.N.A.A.; Abdan, K.; Nasir, N.A.M.; Huseien, G.F. Experimental evaluation and statistical modeling of kenaf fiber-reinforced geopolymer concrete. *Constr. Build. Mater.* **2023**, *367*, 130228. [CrossRef]
72. Makhlouf, M.H.; Abdel-kareem, A.H.; Mohamed, M.T.; El-Gamal, A. Experimental and numerical study of shear strengthening of reinforced concrete beams using jute fiber reinforced polymers (JFRP). *J. Build. Eng.* **2024**, *86*, 108732. [CrossRef]
73. Haddaji, Y.; Majdoubi, H.; Mansouri, S.; Tamraoui, Y.; Manoun, B.; Oumam, M.; Hannache, H. Effect of synthetic fibers on the properties of geopolymers based on non-heat treated phosphate mine tailing. *Mater. Chem. Phys.* **2021**, *260*, 124147. [CrossRef]
74. Dayananda, N.; Keerthi Gowda, B.; Easwara Prasad, G. A study on compressive strength attributes of jute fiber reinforced cement concrete composites. In Proceedings of the IOP Conference Series: Materials Science and Engineering, Moodbidri, India, 2–3 March 2018; p. 012069.
75. Sofat, V.; Khadwal, A.; Meerwal, S. An experimental study to check compressive strength of concrete by using jute fibers as reinforcement. *Int. J. Earth Sci. Eng.* **2017**, *10*, 450–454. [CrossRef]
76. Kim, J.; Park, C.; Choi, Y.; Lee, H.; Song, G. An investigation of mechanical properties of jute fiber-reinforced concrete. *High Perform. Fiber Reinf. Cem. Compos. 6 HPFRCC 6* **2012**, *6*, 75–82.
77. Lewis, G.; Premalal, M. Natural vegetable fibres as reinforcement in cement sheets. *Mag. Concr. Res.* **1979**, *31*, 104–108. [CrossRef]
78. Uzomaka, O.J. Characteristics of akwara as a reinforcing fibre. *Mag. Concr. Res.* **1976**, *28*, 162–167. [CrossRef]
79. Khan, M.; Ali, M. Effect of super plasticizer on the properties of medium strength concrete prepared with coconut fiber. *Constr. Build. Mater.* **2018**, *182*, 703–715. [CrossRef]
80. Khan, M.; Ali, M. Improvement in concrete behavior with fly ash, silica-fume and coconut fibres. *Constr. Build. Mater.* **2019**, *203*, 174–187. [CrossRef]
81. Liu, X.; Wu, T.; Yang, X.; Wei, H. Properties of self-compacting lightweight concrete reinforced with steel and polypropylene fibers. *Constr. Build. Mater.* **2019**, *226*, 388–398. [CrossRef]
82. Ahmad, J.; Majdi, A.; Al-Fakih, A.; Deifalla, A.F.; Althoey, F.; El Ouni, M.H.; El-Shorbagy, M.A. Mechanical and durability performance of coconut fiber reinforced concrete: A state-of-the-art review. *Materials* **2022**, *15*, 3601. [CrossRef]
83. Alomayri, T.; Shaikh, F.; Low, I. Characterisation of cotton fibre-reinforced geopolymer composites. *Compos. Part B Eng.* **2013**, *50*, 1–6. [CrossRef]
84. Alomayri, T.; Low, I.M. Synthesis and characterization of mechanical properties in cotton fiber-reinforced geopolymer composites. *J. Asian Ceram. Soc.* **2013**, *1*, 30–34. [CrossRef]
85. Assaedi, H.; Alomayri, T.; Shaikh, F.U.A.; Low, I. Advances in geopolymer composites with natural reinforcement. In *Advances in Ceramic Matrix Composites*; Elsevier: Amsterdam, The Netherlands, 2018; pp. 461–474.
86. Korniejenko, K.; Frączek, E.; Pytlak, E.; Adamski, M. Mechanical properties of geopolymer composites reinforced with natural fibers. *Procedia Eng.* **2016**, *151*, 388–393. [CrossRef]
87. Das, S.; Sobuz, M.H.R.; Tam, V.W.; Akid, A.S.M.; Sutan, N.M.; Rahman, F.M. Effects of incorporating hybrid fibres on rheological and mechanical properties of fibre reinforced concrete. *Constr. Build. Mater.* **2020**, *262*, 120561. [CrossRef]
88. Zhang, N.; Ye, H.; Pan, D.; Zhang, Y. Effects of alkali-treated kenaf fiber on environmentally friendly geopolymer-kenaf composites: Black liquid as the regenerated activator of the geopolymer. *Constr. Build. Mater.* **2021**, *297*, 123787. [CrossRef]
89. Elsaid, A.; Dawood, M.; Seracino, R.; Bobko, C. Mechanical properties of kenaf fiber reinforced concrete. *Constr. Build. Mater.* **2011**, *25*, 1991–2001. [CrossRef]
90. Wang, X.; He, J.; Mosallam, A.S.; Li, C.; Xin, H. The effects of fiber length and volume on material properties and crack resistance of basalt fiber reinforced concrete (BFRC). *Adv. Mater. Sci. Eng.* **2019**, *2019*, 7520549. [CrossRef]
91. Liu, B.; Zhang, L.Z.; Liu, Q.X.; Ji, T. Study on behaviors of jute fiber reinforced cement based materials. *Appl. Mech. Mater.* **2013**, *253*, 508–511. [CrossRef]
92. Zakaria, M.; Ahmed, M.; Hoque, M.M.; Islam, S. Scope of using jute fiber for the reinforcement of concrete material. *Text. Cloth. Sustain.* **2017**, *2*, 11. [CrossRef]
93. Razmi, A.; Mirsayar, M. On the mixed mode I/II fracture properties of jute fiber-reinforced concrete. *Constr. Build. Mater.* **2017**, *148*, 512–520. [CrossRef]
94. Raval, G.; Kansagra, M. Effects of jute fibers on fiber-reinforced concrete. *Int. J. Innov. Emerg. Res. Eng.* **2017**, *4*, 7–12.
95. Hossain, M.A.; Datta, S.D.; Akid, A.S.M.; Sobuz, M.H.R.; Islam, M.S. Exploring the synergistic effect of fly ash and jute fiber on the fresh, mechanical and non-destructive characteristics of sustainable concrete. *Heliyon* **2023**, *9*, e21708. [CrossRef]
96. Rani, S.Y.; Nusari, M.S.; bin Non, J.; Poddar, S.; Bhaumik, A. Durability of geopolymer concrete with addition of polypropylene fibre. *Mater. Today Proc.* **2022**, *56*, 2846–2851. [CrossRef]
97. Yanou, R.N.; Kaze, R.C.; Adesina, A.; Nemaleu, J.G.D.; Jiofack, S.B.K.; Djobo, J.N.Y. Performance of laterite-based geopolymers reinforced with sugarcane bagasse fibers. *Case Stud. Constr. Mater.* **2021**, *15*, e00762. [CrossRef]
98. Assaedi, H.; Shaikh, F.; Low, I.M. Effect of nanoclay on durability and mechanical properties of flax fabric reinforced geopolymer composites. *J. Asian Ceram. Soc.* **2017**, *5*, 62–70. [CrossRef]
99. Kubba, Z.; Huseien, G.F.; Sam, A.R.M.; Shah, K.W.; Asaad, M.A.; Ismail, M.; Tahir, M.M.; Mirza, J. Impact of curing temperatures and alkaline activators on compressive strength and porosity of ternary blended geopolymer mortars. *Case Stud. Constr. Mater.* **2018**, *9*, e00205. [CrossRef]

100. Mehta, A.; Siddique, R. Strength, permeability and micro-structural characteristics of low-calcium fly ash based geopolymers. *Constr. Build. Mater.* **2017**, *141*, 325–334. [CrossRef]
101. Li, J.; Sun, Z.; Wang, L.; Yang, X.; Zhang, D.; Zhang, X.; Wang, M. Properties and mechanism of high-magnesium nickel slag-fly ash based geopolymer activated by phosphoric acid. *Constr. Build. Mater.* **2022**, *345*, 128256. [CrossRef]
102. Poloju, K.K.; Srinivasu, K. Influence of GGBS and concentration of sodium hydroxide on strength behavior of geopolymer mortar. *Mater. Today Proc.* **2022**, *65*, 702–706. [CrossRef]
103. Zhou, W.; Yan, C.; Duan, P.; Liu, Y.; Zhang, Z.; Qiu, X.; Li, D. A comparative study of high-and low-Al 2 O 3 fly ash based-geopolymers: The role of mix proportion factors and curing temperature. *Mater. Des.* **2016**, *95*, 63–74. [CrossRef]
104. Sitarz, M.; Mozgawa, W.; Handke, M. Vibrational spectra of complex ring silicate anions—Method of recognition. *J. Mol. Struct.* **1997**, *404*, 193–197. [CrossRef]
105. Phair, J.W.; Van Deventer, J.; Smith, J. Mechanism of polysialation in the incorporation of zirconia into fly ash-based geopolymers. *Ind. Eng. Chem. Res.* **2000**, *39*, 2925–2934. [CrossRef]
106. Guo, X.; Shi, H.; Dick, W.A. Compressive strength and microstructural characteristics of class C fly ash geopolymer. *Cem. Concr. Compos.* **2010**, *32*, 142–147. [CrossRef]